Mechanical and Hemodynamic Evaluation of an Adjustable Nitinol Arterial Coupler for Suture-Minimized Microvascular Anastomosis

Allison Rausch[1], BS; Arshiya Chugh[1], BS; Daniel Pies[1], BS; Jacqueline Behring[1], BS; Sofia DeCicco[1], BS

[1]Department of Biomedical Engineering, University of Wisconsin–Madison, Madison, WI, USA

Journal of Reconstructive Microsurgery - Submitted as Academic Coursework BME 402

Abstract

Background Microsurgical arterial anastomosis remains a technically demanding and time-intensive procedure that relies on manual suturing, introducing variability and prolonged ischemia risk. Existing sutureless devices are largely limited to venous systems and are not optimized for the higher pressures and thicker walls of small diameter arteries (2-5 mm). This study evaluates the mechanical feasibility and hemodynamic performance of an adjustable, suture-minimized nitinol arterial coupler designed to improve efficiency while preserving vessel integrity and patency.

Methods A rigid 316L stainless steel prototype was fabricated to evaluate insertion, eversion, alignment, and sealing mechanics prior to development of the final nitinol design. Benchtop testing was performed using ex vivo chicken thigh arteries (2-5 mm). Flow performance was assessed under physiologic pressures (80-120 mmHg) using syringe pump pressurization with dyed fluid to evaluate leakage and patency.

Results Feasibility testing with the 316L stainless steel prototype confirmed successful arterial passage and leak-free flow under test conditions, but revealed limitations in eversion performance, including rollback due to low surface traction. Rollback was significant with smooth stainless steel cuffs (up to 115.3% in arteries and ~20% in veins), but was completely eliminated (0% rollback) using the nitinol spring design due to increased vessel contact points. The spiral cuff demonstrated controlled adjustability, expanding from approximately 2.87 mm to 4.19 mm within the target 2–5 mm vessel range. Overall, results confirm functional feasibility while highlighting the need for improved surface engagement and structural optimization.

Conclusion The proposed arterial coupler demonstrates preliminary mechanical feasibility and hemodynamic safety under physiologic conditions. Identified design refinements will guide optimization of the final nitinol device. With further validation of patency, usability, and mechanical reliability, this system has potential to reduce operative time and improve consistency in microsurgical arterial repair.

Keywords
- Arterial anastomosis
- Self-expanding stent
- Nitinol

1. Introduction

1.1 Motivation and Global Impact

Arterial anastomosis is a fundamental procedure across cardiovascular, transplant, and reconstructive surgeries. It enables vital revascularization in coronary artery bypass grafting, free tissue transfer, trauma repair, and organ transplantation. In the United States alone, over 400,000 coronary artery bypass grafts and tens of thousands of microsurgical reconstructions are performed each year, each relying on precise arterial anastomosis to restore circulation and tissue viability [1]. Despite the importance of arterial anastomosis, manual microsuturing is the only method currently used. Manual microsuturing is highly demanding, time-consuming, and variable between surgeons.

Typical arterial microsuturing requires 30 to 60 minutes of operative time and intensive training to achieve proficiency. Even in expert hands, manual techniques carry approximately an 8% risk of thrombosis, leakage, or anastomotic failure, depending on vessel size and other patient factors [1]. These challenges contribute to prolonged ischemia times which, when exceeding 60 minutes, doubles the likelihood of complications occurring [2].Given its central role across cardiovascular bypass, transplantation, and microsurgical reconstruction, arterial anastomosis is performed at substantial volume across multiple surgical specialties each year [3]. At a global level, an estimated 5 billion people lack access to safe, affordable surgical care, and in sub-saharan Africa there is roughly one reconstructive surgeon per 10 million people, meaning that patients in low-resource or emergency settings often have no access to microsurgical expertise at all [4]. Existing alternatives, such as venous couplers, have demonstrated success in low-pressure venous systems but are not suitable for arteries due to differences in wall thickness, elasticity, and hemodynamic load [5], [6].

Developing a reliable, suture-minimized, expandable arterial coupler addresses these systemic gaps by aiming to streamline the anastomosis process, reduce reliance on surgeon skill, and shorten procedure times. By improving procedural efficiency, this device has the potential to reduce ischemic injury, standardize outcomes, and expand surgical accessibility to a broader range of providers. On a global scale, such technology could broaden access to highly technical microsurgical care, reduce postoperative complications, and ultimately improve survival and recovery rates in patients [7].

The societal implications extend beyond individual operations. Enhancing arterial repair efficiency supports faster trauma response, reduces healthcare resource burden, and enables equitable access to life-saving reconstructive and vascular procedures. A sutureless arterial coupler capable of

maintaining long-term patency and biocompatibility could represent a significant advancement toward safe, efficient, and universally accessible microvascular surgery.

1.2 Current Limitations

Despite its widespread use and clinical importance, arterial anastomosis remains constrained by significant mechanical and procedural limitations. The current reliance on manual microsuturing introduces variability in technique, tension distribution, and suture spacing, all of which directly influence vessel patency and long-term healing. Because small diameter arteries (2-5 mm) are highly sensitive to geometric distortion, even minor misalignment can result in luminal narrowing, disturbed flow, or intimal injury [8].

From a biomechanical perspective, arterial walls are thicker and less compliant than venous structures and are subjected to pulsatile pressures ranging from 80-120 mmHg under normal physiologic conditions, with peaks reaching 160-200 mmHg in hypertensive states [9]. The anastomotic interface must therefore withstand substantial circumferential (hoop) stress while preserving lumen geometry. Inconsistent vessel overlap or uneven compression at the connection site may elevate local wall shear stress, contributing to thrombosis [10]. Maintaining consistent intima-to-intima contact without excessive manipulation is critical for endothelial healing, yet technically difficult to achieve reproducibly.

Another major limitation is procedural time and technical expertise. Extended anastomosis time prolongs ischemia, increasing the risk of tissue necrosis and flap failure [3]. Additionally, the technical demand required to perform microsurgical suturing restricts reproducibility across varying levels of surgical experience. This technical dependency reduces the availability of this procedure in emergency and low-resource settings.

Finally, arteries exhibit variability in diameter, wall thickness, and elasticity across patients and anatomical locations. This physiologic heterogeneity presents a challenge for standardization, as fixed-diameter techniques may cause overstretching in smaller vessels or insufficient fixation in larger ones [7]. Maintaining secure fixation while avoiding intraluminal protrusion or geometric distortion remains a critical design challenge.

Together, these limitations highlight the need for a mechanically stable, adjustable, and reproducible method for arterial anastomosis that preserves hemodynamic integrity while reducing ischemia time and technical burden.

2. Methods

2.1 Overall Design Approach

An iterative engineering design process was used to evaluate the mechanical feasibility of the proposed arterial recoupler device. The design process integrated computer aided design modeling, preliminary structural analysis, feasibility testing, and controlled flow evaluation. A rigid stainless steel tubing prototype was first fabricated to isolate insertion, eversion, alignment, and sealing mechanics prior to introducing adjustability and retention features. Findings from this feasibility phase informed subsequent geometric modifications and the planned fabrication of a nitinol stent based device.

In vitro application of the anastomosis device was practiced on defrosted chicken thighs allocated from various supermarket vendors. There is a degree of variability in the artery diameter when using chicken though, however this is also observed in human arteries and will allow for a metric to measure adjustability in device diameter. Chicken anatomy is consistent to humans based on vessel position, bifurcation, and vessel passing pattern [11].The ischiatic artery, shown in Figure 1, within the chicken leg also has a which has a relatively thicker external diameter and low isolation difficulty making it a more feasible selection for anastomosis testing. Limitations include the lack of hemodynamic circulation, however, this can be resolved by pumping dyed fluid through a cannula.

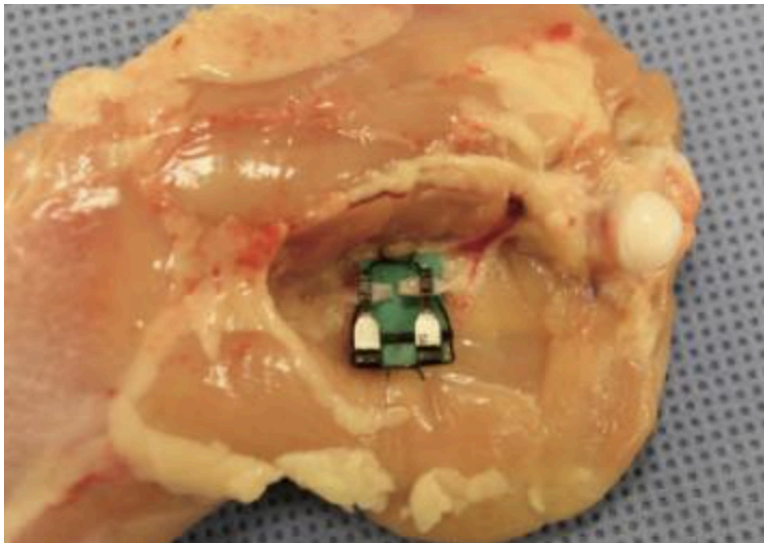

Figure 1. Image of isolated ischiatic artery in lower extremity of chicken [11].

2.2 Rigid Tube Feasibility Prototype

A cylindrical rigid tubing prototype from McMaster was used to evaluate procedural mechanics independent of expansion and retention features. The prototype was fabricated from AISI 316 stainless steel tubing with an inner diameter of 2.31 mm, outer diameter of 2.54 mm, and a height of 3.00 mm. These dimensions were selected to approximate small diameter arterial applications in the 2-5 mm range. This material was selected due to its resistance to corrosion and deformation under physiological conditions and pressures up to 200 mmHg [12].

Unfinished cut edges and manually smoothed edges were the two surface conditions evaluated. Edge smoothing was performed to remove visible burrs and sharp features. This allowed assessment of surface quality influence on vessel handling.

Computer aided design models were created in SolidWorks, shown in Figure 2, to define geometry and confirm dimensional tolerances (see *Appendix V - SolidWorks Modeling Protocol: Rigid Tube* for design steps).

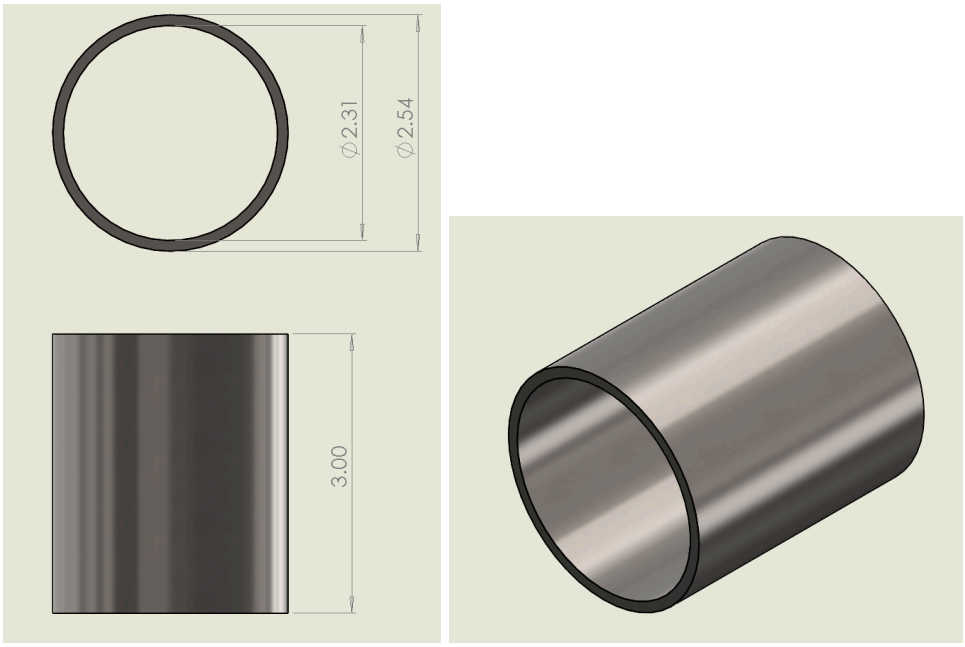

Figure 2. SolidWorks drawing showing the AISI 316 stainless steel rigid tube model used in feasibility testing.

2.3 Insertion & Eversion Testing

Insertion and eversion testing were performed using ex vivo vessel samples within the target diameter range of 2-5 mm. Ex vivo chicken thigh arteries were used as the vessel model. Vessels were

dissected from fresh chicken thighs, and surrounding connective tissue was removed prior to testing. Samples were stored in a freezer and allowed to reach room temperature before experimentation. All testing was conducted under benchtop laboratory conditions at room temperature. The purpose of this testing was to evaluate procedural feasibility and identify mechanical limitations of the rigid prototype.

For insertion testing, the proximal vessel end was advanced through the internal lumen of the rigid stainless steel prototype using microsurgical forceps. After passage, the vessel was inspected visually for tearing, snagging, or surface abrasion. Trials were conducted under two surface conditions: unfinished cut edges and manually smoothed edges. Abrasion was defined as visible disruption of the vessel surface at contact regions. Observations were recorded qualitatively for each trial.

For eversion testing, the vessel end was folded over the external surface of the prototype following insertion. The ability to achieve full circumferential eversion was recorded. Overstretching was assessed by visual inspection. Rollback was defined as partial or complete loss of circumferential engagement without external manipulation. The occurrence of rollback was documented across repeated trials.

2.4 Vessel Alignment Assessment

After eversion of the first vessel, a second vessel end was advanced over the prototype to simulate end to end approximation. Alignment was considered successful if both vessel ends remained circumferentially positioned around the device without visible displacement. Structural rigidity was evaluated based on whether alignment could be achieved without device deformation during handling. Observations were recorded qualitatively.

2.5 Flow Testing

Flow testing was conducted to evaluate sealing performance under controlled pressure conditions. The assembled vessel construct was connected to a syringe pump system to generate steady state flow. Dyed fluid was used to allow visual detection of leakage at the anastomosis interface.

Testing pressures ranged from 80 to 120 mmHg. Additional analysis was performed at a baseline physiologic pressure of approximately 100 mmHg. Leakage was evaluated visually and categorized using a grading scale 0-3, in which Grade 0 indicated no observable leakage and higher grades indicated increasing severity of leakage or structural failure. Surface condition was documented for each trial to assess the influence of edge finishing.

Laminar flow was assumed based on vessel diameter and representative physiologic velocity. A velocity of 0.2 m/s in a 3 mm diameter vessel corresponds to a volumetric flow rate of approximately 84

mL/min. Reynolds number estimates under these conditions fall within the laminar regime for small arteries [13].

2.6 Structural & Hoop Stress Analysis

Preliminary structural analysis was performed using thin wall pressure vessel assumptions. Hoop stress was calculated using the equation:

$$\sigma = \frac{(P \times r)}{t}$$

where P is internal pressure, r is vessel inner radius, and t is vessel wall thickness.

Pressure was set to 100 mmHg and converted to Pascals for calculation [14]. A 3 mm diameter artery was used as the representative model. Arterial wall stress was calculated and compared to reported physiologic ranges of 20 to 100 kPa [15].

For the proposed nitinol design, material properties including yield strength were obtained from published literature. Calculated stresses were compared to the yield strength to confirm that predicted stresses remained within the elastic regime at physiologic pressure [16].

2.7 Planned Quantitative Performance Testing

Following mechanical feasibility testing, additional procedures were defined to evaluate performance metrics relevant to clinical use.

Efficiency testing will measure time to completion of anastomosis from initial vessel handling to final fixation. Timing will be recorded in seconds. Device assisted recoupling will be compared to conventional suturing under the same conditions. Participants will also complete a 5 point Likert scale usability assessment. Failure events will be documented.

Patency and leakage testing will be conducted using syringe pump pressurization between 80 and 120 mmHg. Patency will be defined as continuous flow without occlusion. Leakage will be graded as previously described. Luminal narrowing will be quantified using digital image analysis. Percent stenosis will be calculated as:

$$Percent\ Stenosis = \left(\frac{1 - Minimum\ Lumen\ Diameter}{Reference\ Diameter}\right) \times 100$$

Mechanical integrity testing will be performed using axial tensile loading of the assembled construct. Failure force will be recorded in grams. A minimum pull force threshold of greater than 100 g has been established. Deployment reliability will be assessed by recording misfire rate during repeated trials. Misfire is defined as incomplete deployment or inability to achieve circumferential fixation.

Each of these three experiments will be performed five times by both an experienced surgeon and a relatively inexperienced resident (new to anastomosis). This approach enables evaluation of usability, intuitiveness, and device performance across different levels of surgical experience, while also promoting data reliability and reproducibility.

2.8 Stent Design & Fabrication Plan

An expandable microsurgical stent was designed in SolidWorks, shown in Figure 3, to replace the rigid feasibility prototype (see *Appendix VI - SolidWorks Modeling Protocol: Stent Design* for design steps). The stent geometry was modeled to accommodate arterial diameters ranging from 2 to 5 mm. The design incorporates reduced strut width to improve flexibility and vessel conformity while maintaining sufficient radial support for fixation of everted vessel ends. Key geometric parameters include inner diameter, outer diameter, and strut thickness, which were selected based on prior feasibility testing and physiologic vessel dimensions.

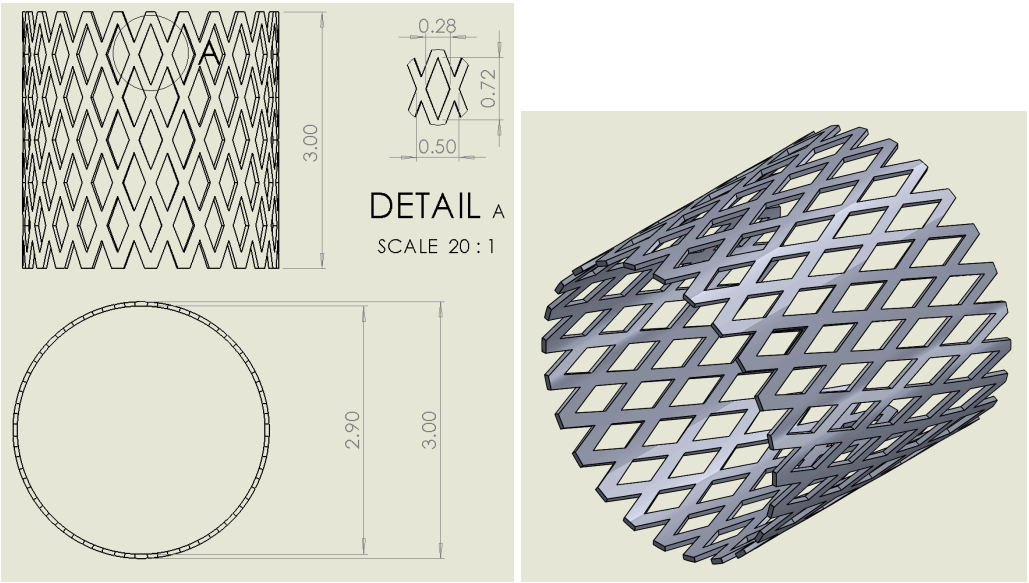

Figure 3. SolidWorks drawing showing the stent model with dimensions.

The device was designed for fabrication in nitinol due to its superelastic properties and established use in endovascular applications. Material selection was based on its ability to undergo radial deformation and recover shape without permanent deformation under physiologic loading conditions [16].

The finalized CAD model was exported in a vendor compatible format and submitted to multiple external manufacturers for feasibility evaluation. Laser cutting was specified as the preferred manufacturing method due to its ability to achieve micro scale geometries and tight tolerances. Electropolishing was also specified to improve surface finish and reduce the risk of vessel damage.

Several vendors reported that the required feature sizes were below their manufacturing capability, while others provided quotes that exceeded budget constraints or could not meet the project timeline. As a result, the nitinol stent was not fabricated and surrogate prototypes were used to evaluate key functional aspects of the design, including radial expansion and vessel retention.

2.9 Surrogate Prototype Development for Concept Validation

Due to cost and manufacturing constraints associated with custom nitinol stents, direct fabrication of the final device was not feasible within the scope of this project. Instead, surrogate prototypes were developed to isolate and experimentally evaluate the key functional mechanisms of the proposed design, including radial expansion, vessel retention, and rollback prevention.

The first surrogate prototype, shown in Figure 4, consisted of a spiral cuff fabricated from stainless steel. This design was used to replicate the adjustable radial expansion behavior of the proposed nitinol stent. A circumferential suture was applied around the cuff to constrain its diameter during insertion and eversion of the vessel. Once the vessel ends were positioned, the suture was released, allowing the cuff to expand outward. This approach enabled controlled evaluation of expansion behavior and vessel accommodation within the target 2-5 mm diameter range.

Figure 4. 3D model of spiral cuff prior to compression.

The second surrogate prototype, shown in Figure 5, utilized a nitinol spring design to model the effects of increased surface interaction and mechanical grip. The spring geometry introduced multiple contact points between the device and the vessel, simulating the effect of microtexturing in the final stent design. This configuration was used to evaluate rollback behavior and assess whether increased surface interaction could improve vessel retention during eversion and alignment.

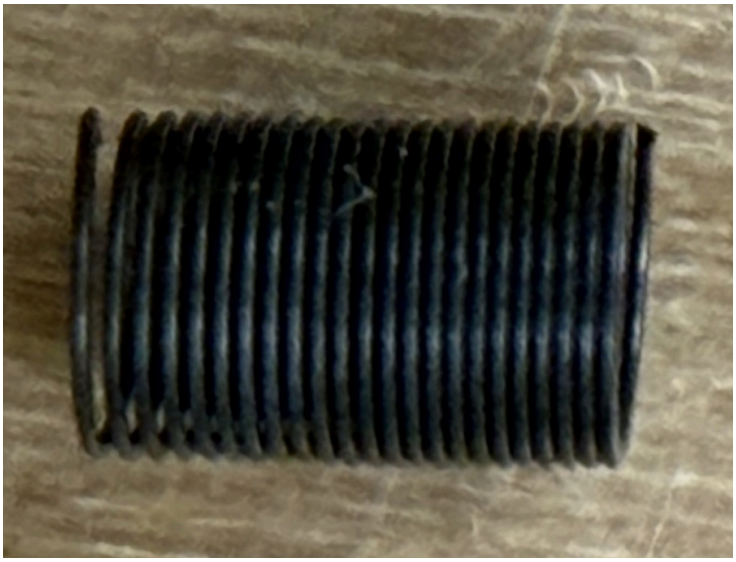

Figure 5. Nitinol spring prototype used to evaluate rollback behavior and increased surface interaction during eversion.

These surrogate prototypes allowed for independent validation of critical design features without requiring fill nitinol fabrication. The spiral cuff was used to assess adjustability and deployment mechanics, while the spring model provided insight into the role of surface interaction in preventing rollback. Together, these models informed the refinement of the final nitinol stent concept and provided experimental validation of its key functionality.

2.10 Spiral Cuff Performance Testing

The spiral cuff surrogate prototype was developed to evaluate the adjustability, leakage performance, and procedural efficiency of the proposed arterial coupler design. The device was fabricated by coiling thin stainless steel strips into a spiral geometry using microsurgical tweezers under magnification to achieve a tight and consistent pitch. Stip thickness was varied between approximately 0.02 mm and 0.05 mm to assess its effect on expansion behavior and mechanical performance.

The uncompressed diameter of the spiral cuff, shown in Figure 6, was measured to be approximately 4.19 mm. During implantation, a circumferential suture was applied to compress the cuff to a reduced diameter of approximately 2.87 mm, allowing for insertion and eversion of the vessel. Once both vessel ends were positioned, the suture was cut to allow controlled expansion of the cuff.

Figure 6. Comparison of cuff diameters in the compressed state (2.87 mm, left) and uncompressed state (4.19 mm, right).

Anastomosis time was recorded from the initial transection of the vessel to the point at which both vessel ends were fully rejoined without further manipulation. These times were compared to a baseline hand sutured anastomosis performed by the client.

Device expansion was quantified using image based measurements. Diameter was recorded in both the compressed and expanded states, and percent expansion was calculated accordingly. Leakage performance was evaluated visually using dyed fluid under physiologic pressure conditions and graded on a 0-3 scale, with Grade 0 indicating no observable leakage.

All trials were conducted using ex vivo vascular specimens obtained from chicken thigh models, including both venous and arterial vessels. Specimen selection was determined by availability during testing sessions conducted under the supervision of surgeons, residents, and medical students. While both vessel types were used, the device was designed for arterial application, and prior testing on arterial tissue demonstrated consistent mechanical behavior. As a result, the inclusion of venous specimens is not expected to significantly impact the evaluation of device performance trends related to expansion, leakage, and procedural workflow.

2.11 Spring Rollback Performance Testing

The spring surrogate prototype was developed to evaluate the effect of increased surface interaction on vessel rollback during eversion. This prototype was used to represent the microtextured retention features proposed for the final nitinol stent design. While the spring was not intended to replicate the final device geometry, its coils provided repeated contact points with the vessel wall, allowing assessment of whether increased surface engagement improved mechanical grip and reduced rollback.

Rollback testing was performed by everting vascular tissue over different cuff materials and measuring the extent of rollback after release. Stainless steel cuffs were tested using both venous and arterial specimens, while nitinol springs were used to evaluate the effect of increased surface interaction and material behavior. Percent rollback was calculated by comparing the displacement of the vessel after release to its initial everted position.

This testing was designed to isolate vessel retention behavior from the full anastomosis workflow, shown in Figures 7-10. These results were used to determine whether microtexturing or similar surface features should be incorporated into the final nitinol stent design to improve stability during eversion and vessel approximation.

Figures 7-10. Spring arterial anastomosis procedure, showing each critical step.

3. Results

3.1 Feasibility Testing Results

Feasibility testing was performed in the client's laboratory using an early prototype fabricated from 316L stainless steel tubing as detailed in Appendix IV. Although Nitinol is the final material for the implant, stainless steel allows for rapid machining and safe handling during testing. This prototype allowed functional evaluation of the device, including artery insertion, eversion performance, and flow behavior, before manufacturing the full Nitinol implant. The stainless steel model was used to confirm geometry, identify sharp edges, and validate the deployment sequence. Evaluated actions and acceptance criteria are summarized in Table 1.

Operation	Acceptance Criteria
Feed artery through rigid tubing	Artery end passes without snagging, tearing, or visible intimal abrasion.
Evert first artery end over tubing	Artery can be everted without tearing or overstretching. No spontaneous rolling back.
Pull opposing artery end over	The second artery can be pulled over the device with ease. The second artery does not roll back once secured on the device.

Operation	Acceptance Criteria
Feed artery through rigid tubing	Artery end passes without snagging, tearing, or visible intimal abrasion.
Evert first artery end over tubing	Artery can be everted without tearing or overstretching. No spontaneous rolling back.
Add fluid flow through device	No leakage at implant site with added flow. Flow remains laminar or minimally disturbed.

Table 1. Operations and associated acceptance criteria evaluated through initial feasibility testing.

The acceptance criteria was defined based on the design specifications for the final device. Ultimately this testing will confirm the stent concept compatibility with 2–5 mm arteries, smooth and safe manipulation, rapid procedural workflow, long-term patency, and the ability to withstand physiologic pressures up to 200 mmHg. The images presented in Figures 11-14 were taken during implantation practice with the client on chicken arteries.

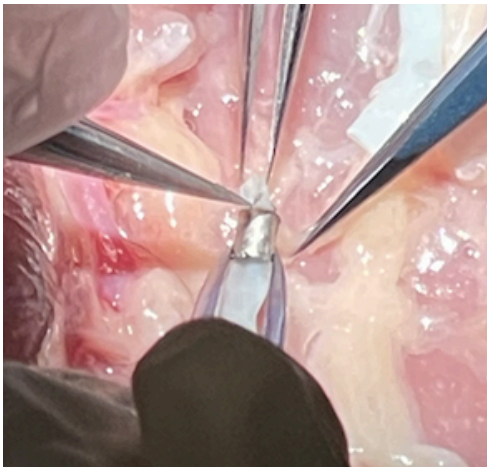

Figure 11. First step of device implantation in which one artery end is pulled through the rigid stent.

The first step in the feasibility testing involved feeding the artery through the rigid tubing at the fixed diameter. In this case, a 3mm chicken artery needed to pass through the 2.31mm inner diameter of the rigid tube. The measurement of the rigid inner diameter is comparable to the 2-2.5mm range the inner

diameter of our machine's nitinol stent will set at. During this operation, there was no visible snagging, tearing, or intimal abrasion on the artery. It was noted that any rough edges do still pose a risk in this step even though no snagging was observed.

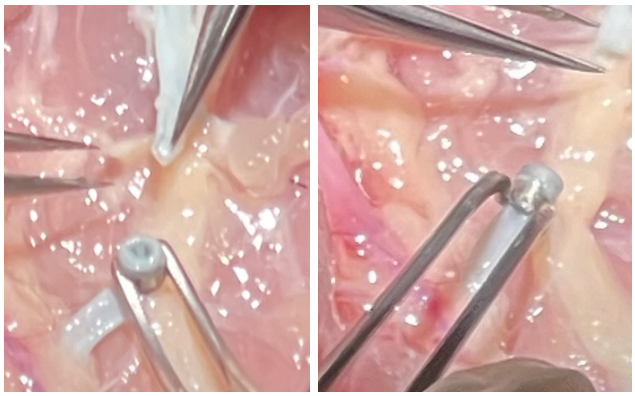

Figure 12. Top view of the inverted artery over the rigid tubing (left) and corresponding side view (right).

The second step was to fully evert the artery over the rigid tubing. A partial failure was observed in this step since the surgeon was able to evert the artery, but only with difficulty. Minor overstretching of the artery end was observed. The outer diameter was too large, requiring more contact with the intima/inner lining of the vessel that is not desired for actual application. The increased intima contact required to evert the artery may contribute to increased thrombogenic risk. The rough cut of the metal tubing also resulted in more substantial abrasions and damage to the other outer lining of the artery making contact with the tubing. A full failure resulted from the inability of the everted artery to stay in place. There was continuous rolling back unless the artery was held manually.

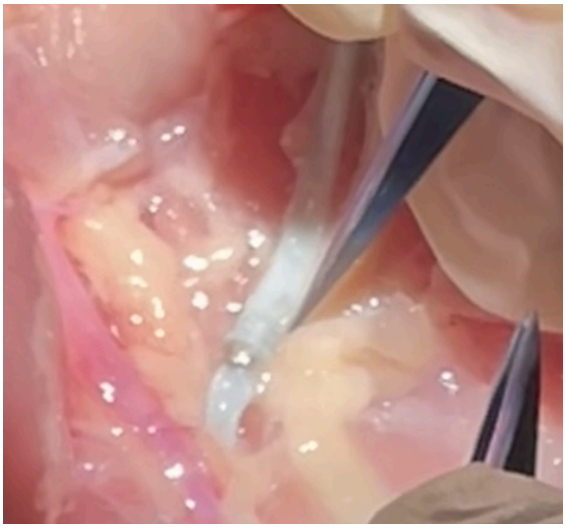

Figure 13. Image of the rigid tube with the everted artery and opposing artery end pulled over the device.

Third, we pulled the opposing artery end over the expanded tubing. Similar issues arose with minor, overstretching and rolling back. More extensive over stretching was observed in this operation now that the outer diameter of the device was increased by the everted artery thickness. The degree of rolling back was reduced now that the artery would make contact with the opposing artery end as opposed to the slippery stainless steel material. Observation from this step further reinforced the need for features that provide better traction during assembly.

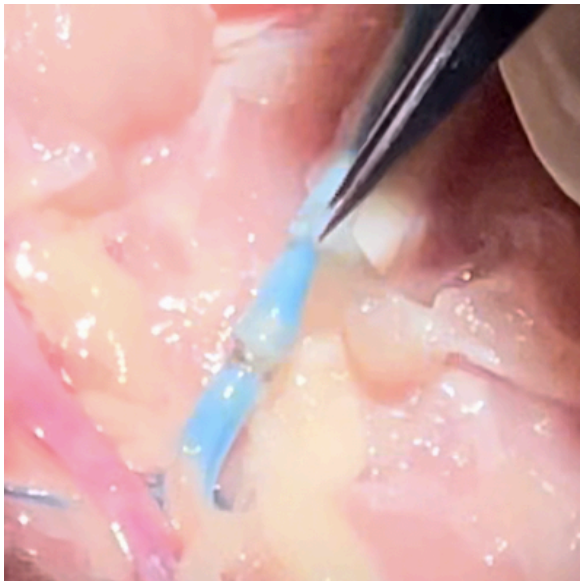

Figure 14. Flow testing of the assembled device showing no visible leakage under applied pressure.

Finally, we performed a flow test to check for leakage and pressure handling. This test fully passed as no leakage was observed over one minute, and flow remained undisturbed, indicating that the concept can support our long-term patency and hemodynamic requirements. The main limitation of this simulation was the flow pressures that were actually achieved. This test did not reach pressures up to our maximum end of 200 mmHg that the device must be able to withstand.

Overall, these feasibility tests validated the core concept while revealing clear targets for the final design revision: improving arterial grip during eversion and decreasing device thickness. Both changes will help us meet our specifications for usability, safety, performance, and manufacturability.

3.2 Spiral Cuff Performance Results

The spiral cuff prototype demonstrated effective performance across adjustability, leakage prevention, and procedural efficiency metrics. The device successfully achieved a compressed diameter of approximately 2.87 mm and expanded to approximately 4.19 mm, remaining within the target vessel range of 2-5 mm. This confirms the ability of the design to accommodate physiologically relevant artery sizes. However, partial rollback was observed during eversion due to the smooth surface finish of the cuff, as illustrated in Figures 15 and 16.

Procedure time decreased significantly across trials, demonstrating a clear learning curve. The initial trial required approximately 4 minutes and 50 seconds, exceeding the baseline hand sutured procedure time of 3 minutes and 55 seconds. However, subsequent trials showed substantial improvement, with the fastest trial completed in approximately 1 minute and 58 seconds. This corresponds to a maximum reduction in procedure time of nearly 50%, indicating strong potential for improved surgical efficiency and usability.

Expansion behavior was dependent on material thickness. The thinner 0.02 mm cuff exhibited limited expansion, while increasing the thickness to 0.05 mm resulted in expansion values in the range of approximately 15-17%. This suggests that increased structural stiffness improves the ability of the device to recover its intended geometry following release of the constraining suture.

Leakage testing showed no observable fluid loss across all trials, corresponding to a leakage grade of 0. Flow remained visually undisturbed, indicating that the device maintained patency and provided an effective seal at the anastomosis site.

Although some trials were conducted on venous specimens due to availability, prior arterial testing demonstrated similar mechanical behavior, supporting the applicability of the results to arterial conditions.

Figure 15-16. Spiral cuff after eversion (left) and partial rollback due to the smooth surface finish (right).

3.3 Spring Model Performance Results

Rollback testing demonstrated a significant improvement in vessel retention with increased surface interaction. Stainless steel cuffs exhibited substantial rollback during eversion, particularly in arterial specimens. Measured rollback values reached up to 115.3% for arteries and ranged between approximately 16-23% for venous specimens. These results indicate that smooth surface materials provide insufficient frictional engagement to maintain stable eversion.

In contrast, the nitinol spring configuration eliminated rollback across all trials, with measured values of 0%. The spring geometry introduced multiple contact points between the device and the vessel wall, increasing surface interaction and resistance to shear forces during eversion. This resulted in consistent retention of the everted vessel without the need for manual support. However, the open coil geometry created gaps along the structure, which prevented sutures from remaining securely in place. During testing, sutures frequently slipped between adjacent coils, limiting the ability to maintain precise positioning and fixation.

The difference in performance between the stainless steel cuffs and nitinol springs highlights the importance of surface interaction in maintaining vessel position. While the spring does not replicate the exact geometry of the final device, it effectively demonstrates that increased surface engagement, such as microtexturing, can significantly improve mechanical stability during the procedure. At the same time, the observed suture instability indicates that a continuous or partially enclosed surface will be necessary in the final design to ensure reliable fixation.

These results directly support the incorporation of microtextured or similar features in the final nitinol stent design to prevent rollback while also maintaining sufficient structural continuity for secure placement and overall procedural reliability.

3.4 SolidWorks Data

SolidWorks fluid-flow simulations were conducted on the arterial-stent configuration under physiological conditions to quantify the hoop stresses generated by transmural pressure. This analysis was used to determine whether the configuration remained within reported physiological stress ranges at normal pressures to identify concentrations within local stress distributions, preventing potential mechanical failure or vessel injury.

To approximate small- to medium-sized human arteries, 3 different 3 mm long segments were used to represent a single arterial wall (wall thickness of 0.5 mm), a nitinol stent with 0.11 mm strut width, and a full stack of artery-stent-artery-artery representing the final state, picture below in Figure 8. Transmural pressure, which is defined as lumen pressure minus external pressure, was set to 100 mmHg to represent typical mean arterial pressure at rest [14]. As defined in the product design specifications, physiologic pressures can rise towards 160-200 mmHg during hypertension or systolic surges, however for simplicity pressure was held constant [15]. Blood flow was given a velocity of 0.2 m/s, which corresponds to approximately 84 mL/min in volumetric flow, and 0.0015 kg/s in mass flow. These values were chosen to be consistent with literature values for small arteries [13].

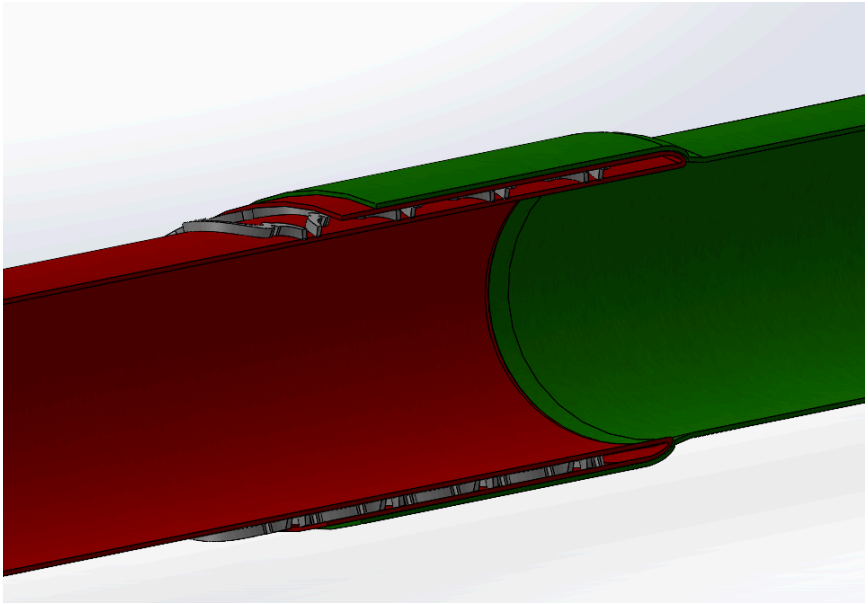

Figure 17. Section view of simulated 3 mm overlapped assembly under 100 mmHg transmural pressure.

It is important to note that while hoop stress can be calculated using the thin-walled cylinder equation, this only provides localized averages, failing to provide geometry and material-specific information. The SolidWorks simulation, however, allows for visualization of stress distributions across local geometry, allowing evaluations of how wall thickness, stent stiffness, and overlapping regions either concentrate or relieve stress.

The simulated hoop stresses closely matched the expected ranges derived from the thin-walled cylinder estimates and literature values. For the single 0.5 mm arterial wall, the SolidWorks model produced a hoop stress of approximately 40 kPa at 100 mmHg, while the isolated nitinol stent configuration produced a hoop stress of approximately 184 kPa at the same pressure. This value represents a model-based estimate, as literature sources typically provide only qualitative or MPa-scale design limits for Nitinol stents rather than quantitative stress data. When the full artery-stent-artery-artery stack was simulated, the average arterial hoop stress was reduced to roughly 53.3 kPa. This indicates that the stacked configuration reduced the load such that the arterial wall was operating within typical single-artery ranges. The implications of these stress values for arterial safety and stent performance are elaborated upon in the Discussion Section.

Wall shear stress was evaluated from the SolidWorks testing simulation alongside the hoop stress analysis. The majority of the areas of highest shear stress appeared along the bowed segments of the artery and near the stent overlap region. These high shear stresses were due to changes in lumen geometry and strut intrusions, which accelerate the flow near the walls of the artery and increase velocity gradients. These locations align with regions that are most typically susceptible to restenosis, drastic changes in geometry or other flow disturbances. These areas, pictured below in Figure 18, support that the simulated shear patterns are consistent with expected hemodynamics of the model.

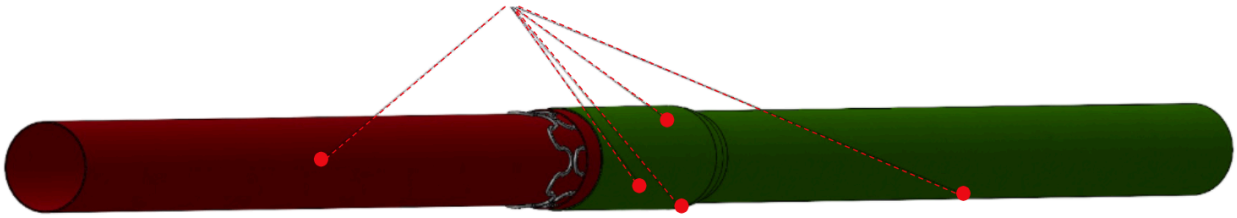

Figure 18. Regions of peak wall shear stress along the artery and stent interface, shown in red.

4. Discussion

The objective of this phase was to evaluate the mechanical feasibility of the proposed arterial recoupler concept using a rigid tubing prototype. Across insertion, eversion, alignment, and flow testing,

the results provided a preliminary validation of the intended procedural workflow while identifying key design limitations to inform subsequent iterations.

Insertion trials demonstrated that vessels consistently passed through the prototype without snagging, tearing, or circumferential deformation which suggests that the overall geometry supports atraumatic guidance. However, localized abrasion was observed at unpolished edges which emphasizes that surface finishing is a critical determinant of insertion safety. When edges were smoothed vessel passage occurred without detectable injury. These findings demonstrate that surface quality rather than geometry alone is the dominant factor governing atraumatic insertion and hence reinforces the importance of electropolishing in the final Nitinol design.

Eversion testing confirmed that the vessel could be folded over the device without excessive overstretching. However it was observed that spontaneous rollback occurred in multiple trials that were conducted. This suggests that while the eversion step is mechanically feasible, the rigid tubing prototype lacks sufficient frictional engagement to maintain stable fixation of the everted vessel ends. The smooth tubing used in this phase provided low surface friction which supports the need for integrated retention features such as micro-texturing or micro-spikes to prevent slippage during the testing trials. Prior studies have shown that controlled surface roughness can enhance tissue-device friction by increasing effective contact area and improving resistance to shear forces at the interface [17]. Rather than relying only on compressive forces, textured surfaces promote greater mechanical engagement with surrounding soft tissue which help to reduce slippage under physiologic conditions. Importantly, when appropriately engineered, these surface modifications can improve fixation stability without causing excessive tissue injury. In the present study, the spontaneous rollback observed during eversion likely reflects low friction between the smooth prototype surface which means that incorporating micro-textured retention features would improve stabilization of the everted vessel ends by increasing grip, supporting more secure alignment during vessel approximation [17].

During approximation of the second vessel, the prototype provided adequate structural rigidity to facilitate alignment without excessive applied force. This confirms the feasibility of the device functioning as a mechanical scaffold to standardize vessel positioning and potentially reducing variability typically associated with manual suturing. Although clinical implementation would likely require supplemental suturing to ensure postoperative security, the device successfully demonstrated its primary role in achieving consistent alignment.

Under steady state flow conditions, the prototype maintained a sealed interface with no observable leakage when edges were smooth, and flow patterns remained laminar. Leakage was observed only in the presence of unfinished or sharp edges which further reinforces the importance of precision manufacturing and surface refinement. Preliminary hoop stress analysis suggested that both the arterial

wall and Nitinol structure operate within mechanically safe limits at physiologic pressures (100 mmHg). Estimated arterial wall stress (~ 40 kPa) falls within reported physiological ranges (20-100 kPa), and calculated Nitinol stress remained well below the material's yield strength. While these results suggest mechanical safety under baseline conditions, performance under elevated pressures requires further evaluation.

Overall, the rigid prototype validated the feasibility of atraumatic insertion, achievable eversion, reproducible alignment, and near leak free flow within the intended workflow. At the same time, the findings highlight the necessity of improved retention features, surface finishing, and precision fabrication to enable successful translation to a functional Nitinol device.

While the initial benchtop testing established mechanical feasibility, the next phase of evaluation expands toward clinical relevance by incorporating usability and hemodynamic performance. Efficiency and usability testing will assess whether the device meaningfully reduces anastomosis time compared to conventional suturing while maintaining acceptable usability scores. A reduction in operative time has significant implications for ischemia duration, surgical fatigue, and overall procedural efficiency. However, improvements in speed must not compromise reliability or vessel integrity. Therefore, timing data will be interpreted alongside failure rates and user reported usability metrics to ensure balanced performance.

Patency and leakage testing using controlled syringe pump pressurization (80-120 mmHg) will provide quantitative validation of sealing performance and luminal preservation. Maintaining a $\geq 95\%$ patency with minimal stenosis (< 20% lumen narrowing) is critical for long-term vessel viability. These metrics will allow for direct comparison with conventional sutured anastomoses and establish whether the device introduces clinically significant geometric narrowing. Furthermore, graded leakage evaluation will help identify failure modes under physiologic and mildly elevated pressures which will inform the refinement of retention and edge design.

If future testing demonstrates acceptable patency, low leakage grades, minimal stenosis, and improved efficiency relative to suturing, the device may represent a viable alternative or adjunct to traditional microvascular techniques. However, additional investigation under elevated pressures, cyclic loading, and eventually in vivo models will be necessary to fully characterize the long term durability and biological response of the device.

4.1 Refined Design Performance and Key Improvements

Following initial feasibility testing, surrogate prototype evaluation provided direct validation of key design improvements targeting adjustability, procedural efficiency, and vessel retention. The spiral cuff design demonstrated that controlled radial expansion could be achieved within the desired two to five

millimeter vessel range using a simple constraint and release mechanism. Expansion behavior was shown to depend on material thickness, with the 0.0508 mm configuration providing improved structural recovery while maintaining sufficient flexibility for vessel eversion.

Procedural efficiency improved significantly across trials, with anastomosis time reduced by up to approximately 50% compared to baseline suturing. This reduction, along with the observed learning curve, supports the design objective of minimizing operative time while maintaining usability across different experience levels such as experts, residents, and medical students. These findings suggest that the device has the potential to reduce ischemia time and improve surgical workflow without increasing technical complexity.

Rollback was identified as a primary failure mode during early feasibility testing due to the insufficient surface interaction between the device and vessel. The spring based surrogate testing demonstrated that increased surface engagement can eliminate rollback entirely, with measured values reduced from over 100% in smooth stainless steel configurations to 0% in Nitinol spring trials. While the spring geometry does not represent the final device, it provides strong evidence that microtextured or similar surface features can significantly improve vessel retention and procedural stability.

These results validate the core functional principles of the proposed nitinol stent design. The combination of controlled expansion, improved surface interaction, and optimized geometry directly addresses the limitations observed in the rigid prototype, resulting in a more stable, efficient, and reliable anastomosis process.

5. Conclusions

Microsurgical arterial anastomosis remains one of the most technically demanding steps in reconstructive surgery, often prolonging operative time and relying heavily on surgeon expertise. Current stent-based solutions lack adaptability and can compromise lumen patency, highlighting the need for a vice that is both efficient and physiologically compatible. This project aimed to address these challenges by designing an adjustable nitinol stent anastomosis device that is capable of guiding two arterial ends into alignment while maintaining patency, reducing variability, and supporting a faster and more consistent surgical workflow.

Initial feasibility testing using a rigid prototype validated the core procedural workflow, including atraumatic insertion, vessel version, alignment, and leak free flow under physiologic conditions. However, key limitations were identified, including insufficient vessel retention and excessive eversion force, which guided subsequent design refinement.

Due to manufacturing and cost constraints associated with custom nitinol fabrication, surrogate prototypes were developed to evaluate the critical functional mechanisms of the final design. Spiral cuss tasting demonstrated that controlled radial expansion within the 2-5 mm vessel range is achievable and that device geometry can be optimized to balance flexibility and structural support. Procedure time was reduced by up to approximately 50% compared to baseline suturing, indicating improved efficiency and a favorable learning curve.

Spring based testing further demonstrated that increased surface interaction can eliminate vessel rollback, reducing a primary failure mode observed in earlier designs. These results provide strong evidence that incorporating microtextured or similar features into the final nitinol stent design will significantly improve retention and procedural stability.

Overall, this work validated the key design principles of an adjustable arterial coupler, including controlled expansion, effective vessel retention, and improved procedural efficiency. While full fabrication and in vivo validation remain necessary, the results of this study represent a critical step toward the development of a clinically viable alternative to traditional microsurgical suturing.

References

[1] G. Pafitanis *et al.*, "Microvascular anastomotic arterial coupling: A systematic review," *J. Plast. Reconstr. Aesthet. Surg.*, vol. 74, no. 6, pp. 1286–1302, Jun. 2021, doi: 10.1016/j.bjps.2020.12.090.

[2] J. A. Arellano *et al.*, "Complications in Prolonged Intraoperative Ischemia Time in Free Flap Breast Reconstruction: A Systematic Review and Meta-Analysis," *Aesthetic Plast. Surg.*, vol. 49, no. 5, pp. 1262–1270, Mar. 2025, doi: 10.1007/s00266-024-04382-7.

[3] D. Ehrl, P. I. Heidekrueger, M. Ninkovic, and P. N. Broer, "Impact of Duration of Perioperative Ischemia on Outcomes of Microsurgical Reconstructions," *J. Reconstr. Microsurg.*, vol. 34, pp. 321–326, Jan. 2018, doi: 10.1055/s-0037-1621729.

[4] H. T. de Berker *et al.*, "Protocol for a systematic review of outcomes from microsurgical free-tissue transfer performed on short-term collaborative surgical trips in low-income and middle-income countries," *Syst. Rev.*, vol. 10, p. 245, Sep. 2021, doi: 10.1186/s13643-021-01797-0.

[5] "Arteries vs. Veins: What's the Difference?" Accessed: Oct. 08, 2025. [Online]. Available: https://www.webmd.com/heart/difference-between-arteries-and-veins

[6] S. A. Khan and R. K. Tayeb, "Postoperative outcomes of aspirin in microvascular free tissue transfer surgery—A systematic review and meta-analysis," *JPRAS Open*, vol. 39, pp. 49–59, Mar. 2024, doi: 10.1016/j.jpra.2023.11.003.

[7] J. G. Ribaudo *et al.*, "Sutureless vascular anastomotic approaches and their potential impacts," *Bioact. Mater.*, vol. 38, pp. 73–94, Apr. 2024, doi: 10.1016/j.bioactmat.2024.04.003.

[8] I. Masson, P. Boutouyrie, S. Laurent, J. D. Humphrey, and M. Zidi, "Characterization of arterial wall mechanical behavior and stresses from human clinical data," *J. Biomech.*, vol. 41, no. 12, pp. 2618–2627, Aug. 2008, doi: 10.1016/j.jbiomech.2008.06.022.

[9] J. Steppan, V. Barodka, D. E. Berkowitz, and D. Nyhan, "Vascular Stiffness and Increased Pulse Pressure in the Aging Cardiovascular System," *Cardiol. Res. Pract.*, vol. 2011, p. 263585, Aug. 2011, doi: 10.4061/2011/263585.

[10] J.-J. Chiu and S. Chien, "Effects of disturbed flow on vascular endothelium: pathophysiological basis and clinical perspectives," *Physiol. Rev.*, vol. 91, no. 1, pp. 327–387, Jan. 2011, doi: 10.1152/physrev.00047.2009.

[11] B. Y. Kang, B.-J. Jeon, K.-T. Lee, and G.-H. Mun, "Comprehensive Analysis of Chicken Vessels as Microvascular Anastomosis Training Model," *Arch. Plast. Surg.*, vol. 44, no. 1, pp. 12–18, Jan. 2017, doi: 10.5999/aps.2017.44.1.12.

[12] E. Messas, M. Pernot, and M. Couade, "Arterial wall elasticity: State of the art and future prospects," *Diagn. Interv. Imaging*, vol. 94, no. 5, pp. 561–569, May 2013, doi: 10.1016/j.diii.2013.01.025.

[13] J. S. Bell *et al.*, “Microstructure and mechanics of human resistance arteries,” *Am. J. Physiol.-Heart Circ. Physiol.*, vol. 311, no. 6, pp. H1560–H1568, Dec. 2016, doi: 10.1152/ajpheart.00002.2016.

[14] K. Neupane and R. T. Jamil, “Physiology, Transpulmonary Pressure,” in *StatPearls*, Treasure Island (FL): StatPearls Publishing, 2025. Accessed: Dec. 10, 2025. [Online]. Available: http://www.ncbi.nlm.nih.gov/books/NBK559004/

[15] “Blood Flow, Blood Pressure, and Resistance | Anatomy and Physiology II.” Accessed: Sep. 15, 2025. [Online]. Available: https://courses.lumenlearning.com/suny-ap2/chapter/blood-flow-blood-pressure-and-resistance-no-content/

[16] D. Stoeckel, A. Pelton, and T. Duerig, “Self-expanding nitinol stents: material and design considerations,” *Eur. Radiol.*, vol. 14, no. 2, pp. 292–301, Feb. 2004, doi: 10.1007/s00330-003-2022-5.

[17] M. Malina, B. Lindblad, K. Ivancev, M. Lindh, J. Malina, and J. Brunkwall, “Endovascular AAA exclusion: will stents with hooks and barbs prevent stent-graft migration?,” *J. Endovasc. Surg. Off. J. Int. Soc. Endovasc. Surg.*, vol. 5, no. 4, pp. 310–317, Nov. 1998, doi: 10.1177/152660289800500404.
D. Stoeckel, A. Pelton, and T. Duerig, “Self-expanding nitinol stents: material and design considerations,” *Eur. Radiol.*, vol. 14, no. 2, pp. 292–301, Feb. 2004, doi: 10.1007/s00330-003-2022-5.

Appendix

Appendix I - Product Design Specification (PDS)

Introduction:

The following table defines important terms used throughout the document (Table 1).

Term	Definition
Anastomosis	An anastomosis is a surgical connection between two structures. It usually means a connection that is created between tubular structures [1].
Ischemia	an inadequate blood supply to an organ or part of the body, especially the heart muscles [2].
Microsurgery	Microsurgery is a surgical discipline that requires precision to repair or rebuild microscopic parts of the body with specialized tools and procedures [3].
Patency	The condition of being open, expanded, or unobstructed.

Table 1: Definitions of terms used throughout the document.

Function:

Microsurgical arterial anastomosis is a cornerstone of reconstructive surgery, enabling tissue transfer and limb salvage. Current techniques are highly time consuming, technically demanding, and are highly dependent on surgeon expertise. Suturing vessels as small as 1 mm can take even the most experienced surgeons 30-60 minutes, extending operating times and jeopardizing tissue viability. Existing stent-based approaches introduce complications by contracting the vessel lumen and lack adaptability across the wide range of vessel diameters encountered in clinical practice. There is a critical need for a biocompatible, adjustable, and easy-to-use device that can reliably reduce operative time while maintaining vessel integrity and minimizing complications.

Client Requirements:

- The client requires that the team's design is adjustable across artery sizes spanning from 2–5 mm in diameter, either through multiple prototypes or a single adjustable device.

- The client requires that the design only interacts with the outer diameter of the artery and avoids intraluminal placement.
- The device should enable completion of arterial anastomosis within 20 minutes.
- The design should be intuitive to operate and require minimal training for experienced or trainee microsurgeons.
- The client requires that the device remain implanted safely for the duration of the patient's life without loss of function or biocompatibility.
- The device must withstand arterial blood pressures up to 160-200 mmHg without deformation, collapse, or fracture.
- The device must be single-use per surgical procedure, compatible with standard sterilization methods and delivered in packaging that maintains sterility until surgical use.
- The device must avoid sharp edges or burrs that could damage vessels, gloves, or surgical personnel.

Design Requirements:

1. Physical and Operational Characteristics

a. *Performance Requirements*

i. This device should be designed for single use per surgical procedure to ensure sterility and consistent performance.

ii. This device must remain implanted in the patient's body for the duration of their lifespan without loss of function or biocompatibility.

iii. This device will enable anastomosis to be completed in less than 20 minutes, as specified by our client, reducing operative time compared to current suturing methods ranging from 30-60 minutes.

1. In head and neck reconstruction, anastomosis time utilizing coupler devices averages 7.5 minutes, compared to 32.2 minutes with sutured techniques [4].

iv. This device must remain effective under ischemic conditions to ensure perfusion is restored before tissue damage occurs.

1. Reperfusion should occur within 5-6 hours of warm ischemia for limb survival, within 3 hours to minimize functional deficits, and within 10-12 hours of cold ischemia under standard preservation methods [5].

v. As specified by the client, the device will function across a vessel range of 2-5 mm with either multiple prototypes to cover this range or one prototype capable of expanding and contracting between sizes.

vi. This device will maintain patency of the vessel lumen by preventing constriction, collapse, or damage to the intima layer.

vii. The device will accommodate variable arterial stiffness, including changes due to age, smoking, or radiation exposure [6].

viii. This device must have a low learning curve when being used by experienced or training microsurgeons, compared to suturing techniques.

ix. This device must be capable of withstanding arterial blood pressures beyond the typical 120/80 mmHg without structural deformation [7]. Extreme arterial blood pressures range from 160-200 mmHg as provided by our client.

x. This device should avoid placements that promote thrombosis, clotting, or inflammatory response. Intraluminal placement should be avoided, but secure fixation of the vessels is crucial.

    1. In head and neck reconstruction, thrombosis occurred in 1.7% of patients with coupler devices, compared to 3.88% with sutured techniques [4].

xi. This device must exhibit corrosion resistance under physiological conditions.

xii. This device must withstand sterilization using ethylene oxide without degradation of material properties or loss of functionality.

b. *Safety*

i. All materials must comply with FDA recognized ISO 10993 standards for biocompatibility, as required for blood-contacting and implantable devices:

    1. Materials must be non-toxic, non-inflammatory, and non-thrombogenic, with no leachable chemicals that could enter systemic circulation [8].

ii. The device must avoid sharp edges, burrs, or protrusions that could puncture gloves, damage arterial walls, or injure handlers.

iii. The device must withstand normal arterial pressures, approximately 120 mmHg, without fracture, collapse, or uncontrolled deformation [9].

iv. The device must be compatible with standard sterilization methods (ethylene oxide, gamma irradiation etc.) [10].

v. Validation of sterilization must follow FDA standards, including demonstrating effective sterilization for complex geometries or multi-layered components [10].

vi. Device packaging must ensure sterility until opened in the surgical field.

vii. Device labeling must include clear labeling for size range compatibility and single-use designation.

c. *Accuracy and Reliability*

i. Patency Rates

1. The device should achieve a minimum patency rate of greater than or equal to 95% immediately post-operation and maintain greater than or equal to 90% patency at 7 days in preclinical animal models. Longer-term patency (>30 days) should remain within clinically acceptable ranges greater than or equal to 85%. Patency is the primary indicator of microsurgical success, reflecting the ability of the anastomosis to maintain unobstructed blood flow. Immediate patency rates with traditional suturing and coupler devices consistently exceed 95%, while long-term rates drop modestly due to thrombosis or intimal hyperplasia. For example, a minimally assisted microsurgical technique achieved 95.1% patency (39/41 anastomoses) immediately post-operation [11]. Similarly, anastomotic coupler devices demonstrated 100% immediate patency with long-term patency rates around 88%. Meeting or exceeding these benchmarks ensures clinical viability [12].

ii. Operative Time Reduction

1. The anastomosis procedure should be completed in less than 20 minutes, representing a 3-6x reduction in operative time compared to hand-sewn sutures (30–60 minutes). Shortening operative time reduces ischemia duration, lowers the risk of flap loss, and improves overall surgical efficiency. Traditional microsuturing of 1 mm vessels can take 30–60 minutes, even for skilled surgeons. In contrast, device-assisted approaches in animal models have demonstrated safe completion in under 5 minutes while maintaining patency [13]. By targeting less than 20 minutes in clinical use, the device balances speed with ease of handling and reliability under realistic surgical conditions.

iii. Vessel Diameter Adaptability

1. The device must reliably function with vessels ranging from 2-3.5 mm in diameter, without causing lumen narrowing greater than 10% compared to the native vessel. Even moderate stenoses can create significant pressure gradients and flow reductions if extended in length, as shown in coronary models [14]. Since resistance to flow increases sharply with small decreases in radius,

maintaining lumen patency is essential in microsurgery where target vessels are only 2-3.5 mm.

iv. Leak Prevention and Structural Integrity

1. Beyond patency, leak prevention is critical to avoiding hematoma formation, which can jeopardize flap survival or limb salvage. Microsurgical studies emphasize the importance of watertight closure, with appropriate suture spacing or coupler alignment to prevent leakage. Experimental work using different suture calibers (8-0 to 11-0) in 1 mm vessels has shown that patency and leak prevention are achievable across a range of technical approaches [15]. A device that reliably seals vessels under physiologic pressures while maintaining lumen integrity directly addresses these clinical requirements.

v. User Consistency and Reliability

1. The device should demonstrate less than a 20% variability in operative time and patency outcomes across different users (beginner vs. experienced microsurgeons) and conditions (artery diameters, variable blood pressures). Current microsurgical success is highly dependent on surgeon expertise and learning curves. Experimental data show significant variability in patency rates across techniques and operators, ranging from 80% to 100% in supermicrosurgical models (0.5–0.8 mm vessels) [16]. By minimizing user-dependent variability, this device should be able to provide consistent performance, reduce training burden, and broaden accessibility of microsurgery to surgeons with less specialized experience.

d. *Life in Service*

i. The anastomotic device must maintain structural integrity and patency for at least 2 weeks post-implantation, supporting the vessel during the critical healing phase [17]. The first two weeks after anastomosis are significant for vessel healing, as new tissue forms and the vessel gradually gains strength. Providing mechanical support during this period reduces the risk of leakage or clot formation, ensuring the vessel can handle normal blood flow once it has regained sufficient structural integrity. Maintaining device support through this early healing phase is essential for patient safety and long-term vessel function.

e. *Shelf Life*

i. The device will be free of any batteries, materials, or solutions that will have a set expiration date. Shelf life will therefore be determined by the sterility of the single-use device and package integrity.

ii. About 50% of medical devices are sterilized with ethylene oxide due to its efficiency in sterilizing a variety of polymers, metals, or ceramics that are muti-layered or have difficult geometries [10]. This will be the main form of sterilization considered for the device's shelf life duration.

iii. Sterility of medical devices exposed to ethylene oxide is at most 5 years [18]. This number is limited by packaging integrity, device material, handling and transportation, and environmental conditions. A minimum shelf life of 3 years will be achieved by considering the following:

1. Storing device in a cool and dry environment to prolong sterility. Condensation within packaging due to high humidity can impact sterility of the device.
    a. Maximum relative humidity of 60% [19].
    b. Temperatures range from 72 to 78 oC [19].
    c. Positive air pressure relationship to adjacent areas [19].
2. Using a sealable and durable package to prevent tears that will eliminate sterile barriers.
3. Devices made from hard plastics and metals are less reactive to moisture and temperature maintaining sterility for longer periods of time. Use of softer more porous materials can reduce shelf life sterility.

f. *Operating Environment*

i. In vivo the device will be exposed and must maintain integrity at the following environmental conditions:

1. Human body temperature is within the range of 36.5-37.5 oC. Irreparable damage to organs can occur when body temperatures are outside of 32.2-41.1 oC [20].
2. Maximum arterial flow pressures can span from 80-120 mmHg for a healthy adult [7]:
    a. Largest arterial pressures during systole is ~120 mmHg due to contraction of the heart that drives blood into arteries.
    b. Largest arterial pressure during diastole is ~80 mmHg due to arterial recoil as the heart fills with blood.
3. Full humidity exposure since the device is continually exposed to blood and interstitial fluid. The device must therefore be resistant to corrosion.

4. Arterial diameters can vary with cardiac output such that any device must accommodate this fluctuation and not be too rigid.

ii. During surgical handling in the operating room, the device may be subject to:

1. Sterilization through ethylene oxide which maintains atmospheric pressure of 101 kPa [21].
2. Operating room temperatures average 20 oC to 24 oC and relative humidity exposure of 40% to 60% [22].
3. Device must be easy to handle across all users wearing surgical gloves and removing device from sterile packaging.

g. *Ergonomic*

i. This device should be designed for comfortable, precise operation by microsurgeons while minimizing hand and wrist fatigue during use. Handles, grips, or controls should accommodate a range of hand sizes and enable natural finger and wrist positions. The device should be balanced and stable, supporting fine motor control and repeatable actions for microsurgical coupling. Materials and textures should enhance grip without causing uncomfortability over extended procedures.

h. *Size*

i. The diameters of designs must range from 2 mm to 5 mm with the initial prototype having a diameter of 3 mm, as specified by the client.

ii. Device diameter must expand approximately 0.3 mm once it is implanted and must remain fixed at the expanded diameter without recoil, collapse, or further expansion, as requested by the client.

i. *Weight*

i. The device should have a mass of approximately 0.5 grams per unit (maximum 1 gram) to minimize risk of vessel tension or displacement. This value is based on preliminary design comparisons and will be validated with bench tests [23].

ii. The device should be comfortably supported by standard microsurgical forceps.

j. *Materials*

i. The device should be manufactured utilizing biocompatible materials approved for surgical use, with properties similar to those found in vascular stents. Suitable materials include 316 L stainless steel or Nitinol [24].

1. The design may incorporate a balloon expansion mechanism for adjustable sizing, composed of materials such as nylon or polyethylene terephthalate [25].

ii. The material will be flexible and durable to accommodate variable vessel sizes while maintaining its structure to prevent constriction or collapsation under varying physiological pressures.

iii. The selected material will not contact the arterial lumen, as intraluminal components increase the risk of thrombosis and immune response.

iv. Reabsorbable or dissolvable materials may be considered for future iterations, but are not required for the initial prototype:

1. Drug eluting stents (DES) and resorbable biodegradable stents (RBS) are currently utilized throughout clinical trials. Rapamycin and Paclitaxel are embedded in a polymer matrix coated onto stent wires and released from DES to inhibit the proliferation of smooth muscle cells and reduce restenosis [26].

k. *Aesthetics, Appearance, and Finish*

i. The device should have a professional, modern appearance that conveys quality and precision appropriate for a surgical environment.

ii. Finishes should be smooth, easily sanitizable, and resistant to staining and corrosion.

iii. Components should also be visually consistent with colors and materials that support intuitive use.

2. Production Characteristics

a. Quantity

i. This device is intended to be a single use unit per procedure in order to maintain sterility and consistent performance.

ii. A single prototype will be fabricated by the end of the first month to demonstrate feasibility. Four prototypes covering the 2-5 mm arterial range will be manufactured by the end of the semester.

b. *Target Product Cost*

i. Product cost and manufacturing will not exceed the $1,000 budget allotted by the client.

ii. Current venous couplers on the market span from $250 - $400 per single-use device [27].

3. Miscellaneous

a. *Standards and Specifications*

i. Current Microvascular Anastomotic Coupler Devices on the market are classified as Class II medical devices:

1. The regulatory controls for Class II devices include general controls, special controls, and premarket notification 510(k). If the proposed composition of the biomaterial is substantially equivalent to a predicate device that is active on the market it can gain approval. If not, clinical trials are required for premarket approval [28].

ii. The International Organization for Standardization (ISO) has a couple of standards that apply to the development of an arterial anastomosis device:

1. ISO10993 guarantees biological compatibility of a medical device- ensuring nontoxic, nonthrombogenic, noncarcinogenic, and nonmutagenic effects on the biological system [29].
2. ISO13485 requires that medical devices are monitored by quality management systems. Objective of the standard ensures production of a medical device and related services that meet customer requirements consistently [30].
3. ISO14971 applies risk management monitoring to the design, manufacturing, and life cycle of a medical device [31].
4. ISO11135 monitors the sterility and packaging requirements for the device being exposed to ethylene oxide sterilization [32].

b. *Customer*

i. Dr. Jasmine Craig, MD, PhD, is a plastic surgery resident in the Department of Surgery at the University of Wisconsin-Madison School of Medicine and Public Health. Dr. Craig's clinical insights ensure the device aligns with surgical workflows and addresses real-world challenges in vascular reconstruction [33].

ii. Dr. Weifeng Zeng, MD, is an assistant scientist and microsurgical instructor at the University of Wisconsin-Madison. Dr. Zeng contributes his expertise in microsurgical education and simulation to the project, providing valuable feedback on the device's usability and potential integration into training curriculum [34].

c. *Patient Related Concerns*

i. The device must minimize the risk of blood clot formation and platelet adhesion at the vessel interface during use. Blood is the first tissue to interact with an implanted device, and protein layers that form on the device surface can trigger platelet adhesion and clot formation. Device surfaces with appropriate chemical and physical properties such as hydrophilicity, neutral charge, and specific functional groups can reduce these interactions and lower the risk of thrombosis. This is critical for patient safety and

long-term device performance, ensuring that the device can remain in place without causing adverse blood reactions [35].

d. *Competition*

i. The GEM Microvascular Anastomotic Coupler, produced by Synovis Micro Companies Alliance (Baxter), is the most widely used commercial coupler system in microsurgery [36]. The device uses two interlocking polyethylene rings with pins that evert and appose vessel ends. Clinical studies report high venous patency rates and reduced operative time compared to hand-sewn sutures [37]. However, the device is limited to low-pressure venous systems and is not suitable for arteries due to their thicker, more elastic walls and higher intraluminal pressures, which increase the risk of thrombosis and device failure [38]. In small arteries, practical limitations include ring bulk in tight fields and limited adaptability across small diameter ranges.

ii. Magnetic Compression Anastomosis (MCA) devices use paired rare-earth magnets to approximate tissue via controlled compression [39]. The UCSF Magnamosis platform demonstrates bowel anastomoses with magnet-mediated tissue fusion, and in 2024 the MagDI system received FDA De Novo classification for gastrointestinal (GI) duodeno-ileal anastomosis [40], [41]. Current MCA device sizes are fit for GI lumens but not scalable to 2-5 mm arteries. Other concerns with these devices include potential for misalignment and anastomotic stricture/stenosis [42].

iii. External Cuff techniques evert a vessel end over a short tube/collar and insert it into the opposing end, eliminating sutures and standardizing apposition [43]. Polyethylene cuffs show feasibility in sub-millimeter animal vessels and outline practical construction and handling [44]. Intraluminal approaches, including nickel-titanium (NiTi) shape-memory micro-stents, provide radial support from within and can shorten anastomosis time in preclinical models [45], [46]. The US 575,5772A patent describes a radially expansive vascular prosthesis using a heat-memory alloy ring, while US 9,642,623 B2 outlines an external coupler system designed to secure vessel ends without intraluminal components [47], [48]. However, systematic reviews document recurring drawbacks including reduced compliance at the junction, risks of stenosis or leakage, and potential endothelial injury and hemodynamic disturbance at the interface [49], [50].

iv. A dissolvable sugar-based stent has been proposed as an intra-operative scaffold to hold vessel ends during suturing and then dissolve within 4-8 minutes once flow is restored [51]. This approach addresses handling and speed but is not implantable and lacks arterial in-vivo durability data. Patents such as US 10,285,702B2 and US 20,110,106,118A1

describe absorbable or degradable coupler devices/scaffolds for vascular and microvascular anastomosis [52], [53]. These filings similarly emphasize temporary mechanical support with programmed degradation. However, concerns of degradation rate, mechanical strength during load, and the safety of by-products remains [54].

v. Recent intellectual property (IP) and preclinical work focuses on external/self-expanding couplers, shape-memory alloy (NiTi) rings, and bioresorbable scaffolds for sutureless vascular connections. Most remain pre-clinical, with key open questions on diameter control and compliance matching in smaller diameter arteries and degradation rate/by-product safety over the healing window.

References

[1] "Anastomosis: MedlinePlus Medical Encyclopedia." Accessed: Sept. 15, 2025. [Online]. Available: https://medlineplus.gov/ency/article/002231.htm

[2] "What Is Ischemia?," WebMD. Accessed: Sept. 17, 2025. [Online]. Available: https://www.webmd.com/heart-disease/what-is-ischemia

[3] "What Is Microsurgery?," Cleveland Clinic. Accessed: Sept. 15, 2025. [Online]. Available: https://my.clevelandclinic.org/health/treatments/microsurgery

[4] C. Ohayon et al., "Efficiency and outcomes in microvascular anastomosis: A meta-analysis of mechanical versus manual techniques," J. Cranio-Maxillofac. Surg., vol. 53, no. 10, pp. 1720–1730, Oct. 2025, doi: 10.1016/j.jcms.2025.07.015.

[5] A. Chakradhar, J. Mroueh, and S. G. Talbot, "Ischemia Time in Extremity Allotransplantation: A Comprehensive Review," Hand N. Y. N, p. 15589447241287806, Nov. 2024, doi: 10.1177/15589447241287806.

[6] J. Steppan, V. Barodka, D. E. Berkowitz, and D. Nyhan, "Vascular Stiffness and Increased Pulse Pressure in the Aging Cardiovascular System," Cardiol. Res. Pract., vol. 2011, p. 263585, Aug. 2011, doi: 10.4061/2011/263585.

[7] "Blood Flow, Blood Pressure, and Resistance | Anatomy and Physiology II." Accessed: Sept. 15, 2025. [Online]. Available: https://courses.lumenlearning.com/suny-ap2/chapter/blood-flow-blood-pressure-and-resistance-no-content/

[8] C. for D. and R. Health, "Use of International Standard ISO 10993-1, 'Biological evaluation of medical devices - Part 1: Evaluation and testing within a risk management process.'" Accessed: Sept. 15, 2025. [Online]. Available:

https://www.fda.gov/regulatory-information/search-fda-guidance-documents/use-international-standard-iso-10993-1-biological-evaluation-medical-devices-part-1-evaluation-and

[9] L. R. Aug 14 and 2025, “Understanding Blood Pressure Readings,” www.heart.org. Accessed: Sept. 15, 2025. [Online]. Available: https://www.heart.org/en/health-topics/high-blood-pressure/understanding-blood-pressure-readings

[10] C. for D. and R. Health, “Sterilization for Medical Devices,” FDA, May 2025, Accessed: Sept. 15, 2025. [Online]. Available: https://www.fda.gov/medical-devices/general-hospital-devices-and-supplies/sterilization-medical-devices

[11] G. Sert, “Safe, fast, and minimally-assisted microsurgical anastomosis with combined open-loop suturing and airborne tying: a clinical and experimental study,” Turk. J. Trauma Emerg. Surg., 2023, doi: 10.14744/tjtes.2023.79702.

[12] T. T. Mai, L. T. T. Nguyen, and P. D. Nguyen, “Efficiency and safety of microvascular anastomotic coupler for wrist revascularization in traumatic injuries,” JPRAS Open, vol. 41, pp. 252–259, Sept. 2024, doi: 10.1016/j.jpra.2024.06.017.

[13] S. An et al., “Biocompatibility and patency of a novel titanium vascular anastomotic device in a pig jugular vein,” Sci. Rep., vol. 11, no. 1, p. 17512, Sept. 2021, doi: 10.1038/s41598-021-97157-y.

[14] R. L. Feldman, W. W. Nichols, C. J. Pepine, and C. R. Conti, “Hemodynamic significance of the length of a coronary arterial narrowing,” Am. J. Cardiol., vol. 41, no. 5, pp. 865–871, May 1978, doi: 10.1016/0002-9149(78)90726-9.

[15] Y. Zheng, J. J. Corvi, J. R. Paladino, and Y. Akelina, “Smoothing the steep microsurgery learning curve: considering alternative suture sizes for early-stage microsurgery training with in vivo rat models,” Eur. J. Plast. Surg., vol. 44, no. 6, pp. 733–737, Dec. 2021, doi: 10.1007/s00238-021-01850-0.

[16] V.-A. Ratoiu et al., “Supermicrosurgical Vascular Anastomosis—A Comparative Study of Lumen-Enhancing Visibility Techniques,” J. Clin. Med., vol. 14, no. 2, p. 555, Jan. 2025, doi: 10.3390/jcm14020555.

[17] R. B. Morgan and B. D. Shogan, “The science of anastomotic healing,” Semin. Colon Rectal Surg., vol. 33, no. 2, p. 100879, June 2022, doi: 10.1016/j.scrs.2022.100879.

[18] “What Is the Duration of Ethylene Oxide Sterilization Effectiveness?,” https://www.sterility.com/. Accessed: Sept. 15, 2025. [Online]. Available: https://www.sterility.com/how-long-does-ethylene-oxide-sterilization-last/

[19] “Temperature and Humidity Requirements – Guidance for Storage of Sterile Supplies | Joint Commission.” Accessed: Sept. 15, 2025. [Online]. Available:

https://www.jointcommission.org/en-us/knowledge-library/support-center/standards-interpretation/standards-faqs/000001275

[20] V. E. Del Bene, “Temperature,” in Clinical Methods: The History, Physical, and Laboratory Examinations, 3rd ed., H. K. Walker, W. D. Hall, and J. W. Hurst, Eds., Boston: Butterworths, 1990. Accessed: Sept. 15, 2025. [Online]. Available: http://www.ncbi.nlm.nih.gov/books/NBK331/

[21] “EtO Sterilization: Principles of Process Design.” Accessed: Sept. 15, 2025. [Online]. Available: https://www.mddionline.com/design-engineering/eto-sterilization-principles-of-process-design

[22] G. Deiana et al., “Ten-Year Evaluation of Thermal Comfort in Operating Rooms,” Healthcare, vol. 10, no. 2, p. 307, Feb. 2022, doi: 10.3390/healthcare10020307.

[23] Q. Lu et al., “End-to-end vascular anastomosis using a novel magnetic compression device in rabbits: a preliminary study,” Sci. Rep., vol. 10, no. 1, p. 5981, Apr. 2020, doi: 10.1038/s41598-020-62936-6.

[24] F. Hoseini, A. Bellelli, L. Mizzi, F. Pecoraro, and A. Spaggiari, “Self-expanding Nitinol stents for endovascular peripheral applications: A review,” Mater. Today Commun., vol. 41, p. 111042, Dec. 2024, doi: 10.1016/j.mtcomm.2024.111042.

[25] I. Rykowska, I. Nowak, and R. Nowak, “Drug-Eluting Stents and Balloons—Materials, Structure Designs, and Coating Techniques: A Review,” Molecules, vol. 25, no. 20, p. 4624, Oct. 2020, doi: 10.3390/molecules25204624.

[26] D. H. Kohn and J. E. Lemons, “Appendix C - Chemical Composition of Metals and Ceramics Used for Implants,” in Biomaterials Science (Fourth Edition), W. R. Wagner, S. E. Sakiyama-Elbert, G. Zhang, and M. J. Yaszemski, Eds., Academic Press, 2020, pp. 1531–1532. doi: 10.1016/B978-0-12-816137-1.15003-2.

[27] “In-Date Baxter Anastomotic Coupler GEM2752/I box of 1... - Synergy SurgicalTM.” Accessed: Sept. 15, 2025. [Online]. Available: https://www.synergysurgical.com/product/0-in-date/84-baxter/1714-anastomotic-coupler/46233100-synovis-gem-coupler-2.0mm-GEM2752I/?srsltid=AfmBOordjGQjoG1aP9tuME-z8lvb0_nGYjxdCnTogz4OpcMpM_tDq0Mr

[28] C. for D. and R. Health, “Classify Your Medical Device,” FDA. Accessed: Sept. 17, 2025. [Online]. Available: https://www.fda.gov/medical-devices/overview-device-regulation/classify-your-medical-device

[29] B. Huzum et al., “Biocompatibility assessment of biomaterials used in orthopedic devices: An overview (Review),” Exp. Ther. Med., vol. 22, no. 5, p. 1315, Nov. 2021, doi: 10.3892/etm.2021.10750.

[30] “ISO 13485,” Amtivo US. Accessed: Sept. 17, 2025. [Online]. Available: https://amtivo.com/us/iso-certification/iso-13485/

[31] "ISO 14971 Risk-Management Compliance Quick Guide," MasterControl. Accessed: Sept. 17, 2025. [Online]. Available: https://www.mastercontrol.com/resource-center/documents/iso-14971-2019-compliance-requirements

[32] "ISO 11135:2014," ISO. Accessed: Sept. 17, 2025. [Online]. Available: https://www.iso.org/standard/56137.html

[33] "Jasmine Craig," Department of Surgery. Accessed: Sept. 15, 2025. [Online]. Available: https://www.surgery.wisc.edu/staff/jasmine-peters/

[34] M. Education, "Microsurgery Education," Microsurgery Education. Accessed: Sept. 15, 2025. [Online]. Available: https://microsurgeryeducation.org/meet-the-team-2

[35] L.-C. Xu, J. W. Bauer, and C. A. Siedlecki, "Proteins, platelets, and blood coagulation at biomaterial interfaces," Colloids Surf. B Biointerfaces, vol. 124, pp. 49–68, Dec. 2014, doi: 10.1016/j.colsurfb.2014.09.040.

[36] "Microvascular Anastomotic Coupler | Microvascular Anastomosis Couplers." Accessed: Sept. 15, 2025. [Online]. Available: https://www.synovismicro.com/html/products/gem_microvascular_anastomotic_coupler.html

[37] J. G. Ribaudo et al., "Sutureless vascular anastomotic approaches and their potential impacts," Bioact. Mater., vol. 38, pp. 73–94, Apr. 2024, doi: 10.1016/j.bioactmat.2024.04.003.

[38] "Synovis Surgical, a division of Baxter, licenses Arterial Everter transplant surgery technology from U-M," UM - Innovation Partnerships. Accessed: Sept. 15, 2025. [Online]. Available: http://innovationpartnerships.umich.edu/stories/synovis-surgical-a-division-of-baxter-licenses-arterial-everter-transplant-surgery-technology-from-u-m/

[39] M.-M. Zhang et al., "Magnetic compression anastomosis for reconstruction of digestive tract after total gastrectomy in beagle model," World J. Gastrointest. Surg., vol. 15, no. 7, pp. 1294–1303, July 2023, doi: 10.4240/wjgs.v15.i7.1294.

[40] "Magnamosis | Surgical Innovations." Accessed: Sept. 15, 2025. [Online]. Available: https://surgicalinnovations.ucsf.edu/magnamosis

[41] "Device Classification Under Section 513(f)(2)(De Novo)." Accessed: Sept. 17, 2025. [Online]. Available: https://www.accessdata.fda.gov/scripts/cdrh/cfdocs/cfpmn/denovo.cfm?id=DEN240013&utm_source=chatgpt.com

[42] T. Kamada et al., "New Technique for Magnetic Compression Anastomosis Without Incision for Gastrointestinal Obstruction," J. Am. Coll. Surg., vol. 232, no. 2, pp. 170-177.e2, Feb. 2021, doi: 10.1016/j.jamcollsurg.2020.10.012.

[43] D. J. Coleman and M. J. Timmons, "Non-suture external cuff techniques for microvascular

anastomosis," Br. J. Plast. Surg., vol. 42, no. 5, pp. 550–555, Sept. 1989, doi: 10.1016/0007-1226(89)90043-X.

[44] T. F. Fensterer, C. J. Miller, G. Perez-Abadia, and C. Maldonado, "Novel Cuff Design to Facilitate Anastomosis of Small Vessels During Cervical Heterotopic Heart Transplantation in Rats," Comp. Med., vol. 64, no. 4, pp. 293–299, Aug. 2014.

[45] N. Saegusa et al., "Sutureless microvascular anastomosis assisted by an expandable shape-memory alloy stent," PLOS ONE, vol. 12, no. 7, p. e0181520, July 2017, doi: 10.1371/journal.pone.0181520.

[46] P. Senthil-Kumar et al., "An intraluminal stent facilitates light-activated vascular anastomosis," J. Trauma Acute Care Surg., vol. 83, no. 1 Suppl 1, pp. S43–S49, July 2017, doi: 10.1097/TA.0000000000001487.

[47] J. P. Agarwal, B. K. Gale, L. Nguyen, C. Shorr, B. Stauffer, and C. L. Gehrke, "Methods, devices and apparatus for performing a vascular anastomosis," US9642623B2, May 09, 2017 Accessed: Sept. 15, 2025. [Online]. Available: https://patents.google.com/patent/US9642623B2/un

[48] M. A. Evans and G. A. Watanabe, "Radially expansible vascular prosthesis having reversible and other locking structures," US5755772A, May 26, 1998 Accessed: Sept. 15, 2025. [Online]. Available: https://patents.google.com/patent/US5755772/en

[49] J. G. Ribaudo et al., "Sutureless vascular anastomotic approaches and their potential impacts," Bioact. Mater., vol. 38, pp. 73–94, Aug. 2024, doi: 10.1016/j.bioactmat.2024.04.003.

[50] D. P. Mallela et al., "A systematic review of sutureless vascular anastomosis technologies," Semin. Vasc. Surg., vol. 34, no. 4, pp. 247–259, Dec. 2021, doi: 10.1053/j.semvascsurg.2021.10.004.

[51] A. Farzin et al., "3D printed sugar-based stents facilitating vascular anastomosis," Adv. Healthc. Mater., vol. 7, no. 24, p. e1800702, Dec. 2018, doi: 10.1002/adhm.201800702.

[52] D. G. Son, J. H. Kim, K. C. Choi, and S. H. Song, "Absorbable vascular anastomotic system," US20110106118A1, May 05, 2011 Accessed: Sept. 15, 2025. [Online]. Available: https://patents.google.com/patent/US20110106118A1/en

[53] R. R. Jose, W. K. Raja, D. L. Kaplan, A. Ibrahim, S. Lin, and A. Abdurrob, "Bioresorbable biopolymer anastomosis devices," US10285702B2, May 14, 2019 Accessed: Sept. 15, 2025. [Online]. Available: https://patents.google.com/patent/US10285702B2/en?oq=US+10%2c285%2c702

[54] L. Mao et al., "Structural Design of Biodegradable Mg Gastrointestinal Anastomosis Staples for Corrosion and Mechanical Strength Analysis," ACS Appl. Bio Mater., vol. 8, no. 4, pp. 3404–3415, Apr. 2025, doi: 10.1021/acsabm.5c00143.

Appendix II - Material Costs and Analysis

Item	Description	Manufacturer	Mft Pt#	Vendor	Vendor Cat#	Date	QTY	Cost Each	Total	Link
304 Stainless Steel Tubing	Miniature, 0.12" OD, 0.01" Wall Thickness - Length 1'	McMaster-Carr	8987K24	McMaster-Carr	8987K24	12/04/2025	1	$8.17	$8.17	Link
304 Stainless Steel Tubing	Miniature, 0.109" OD, 0.012" Wall Thickness - Length 2"	McMaster-Carr	5560K655	McMaster-Carr	5560K655	12/04/2025	1	$4.49	$4.49	Link
304 Stainless Steel Tubing	Miniature, 0.1" OD, 0.009" Wall Thickness - Length 1'	McMaster-Carr	8988K23	McMaster-Carr	8988K23	12/04/2025	1	$9.93	$9.93	Link
KRL Nitinol Micro-Spring	5 mm length, 0.5 mm diameter micro-spring	Kellogg's Research Lab	898J402	Kellogg's Research Lab	N/A	2/25/2026	1	$12.99	$12.99	Link
KRL Nitinol Microsprings	Varying Mandrel sizes (mm): 0.5, 0.9, 1.15, 1.6	Kellogg's Research Lab	5450K752	Kellogg's Research Lab	N/A	3/23/2026	4	$8.00	$36.99	Link
Metal Shim Kit	Metal shim kit with sheets of stainless steel of varying thicknesses	Afoxos	N/A	Home Depot	2-HDPH005OT053	3/24/2026	1	$50.30	$50.30	Link
								TOTAL:	**$122.87**	

Appendix III - Design Matrix

Date: September 26, 2025

Advisor: Professor Suarez-Gonzalez
Client: Dr. Jasmine Craig
Lab Section: 308
Team Members:

- Allison (Ally) Rausch (Team Leader)
- Sofia Decicco (BWIG)
- Daniel Pies (BSAC)
- Arshiya (Ria) Chugh (BPAG)
- Jacqueline (Jackie) Behring (Communicator)

Design Matrix:

		Design 1: Sock Clamp 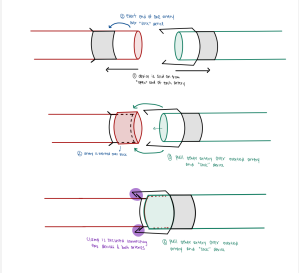		**Design 2: Expandable Stent** 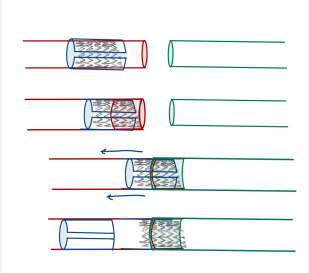		**Design 3: SpikeStent** 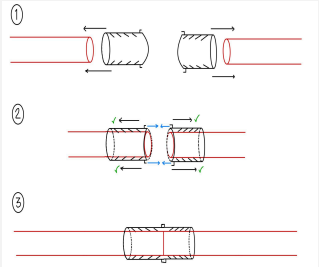	
Criteria	Weight	Score	Weighted Score	Score	Weighted Score	Score	Weighted Score
Efficiency	25	3	15	4	20	2	10
Adjustability	20	1	4	4	16	1	4
Intima Contact	15	5	15	5	15	2	6
Durability	15	4	12	3	9	3	9
Safety	10	4	8	4	8	2	4
Manufacturability	10	4	8	3	6	3	6
Cost	5	4	4	3	3	4	4
Total (Out of 100):		66		77		43	

Criteria Descriptions:

Efficiency: Efficiency will be evaluated based on the total time required to implant the device, starting the moment the artery is clamped off and ending when blood flow is successfully reestablished. Because prolonged ischemia can lead to tissue damage, minimizing implantation time is the most critical factor in the success of this device. Per client requirements, the implantation time should be at most 20 seconds.

Adjustability: Adjustability refers to the device's ability to fit securely across a range of arterial diameters. As specified by the client, the preferred design should be pre-set to an intended diameter but capable of expanding dynamically in response to arterial flow and pressure. This feature ensures compatibility with patient-specific anatomies and allows the device to adapt to physiological changes, ultimately reducing the risk of leakage and clotting.

Intima Contact: The degree of intima-to-intima contact between the joined arteries will be a major factor in ranking device performance. Strong and uniform contact is essential for promoting endothelial healing and reducing the risk of thrombosis. Sustained arterial contact is directly tied to long-term patency and patient rehabilitation.

Durability: Durability will be evaluated based on the device's ability to withstand the body's environmental conditions and maintain structural integrity during the operation, preserving required physical properties over its intended lifetime. This includes resistance to fatigue, corrosion, and degradation.

Safety: Safety will be ranked on how likely an injury is to occur during implantation and how likely the device is to harm the patient while implanted. This includes risks such as vessel tearing, clot formation, inflammation, or immune response. The safest designs will minimize sharp edges, toxic materials, or complex deployment mechanisms that increase the chance of adverse outcomes.

Manufacturability: Manufacturability measures how easily and cost-effectively the device can be produced using available materials, processes, and technologies. This includes fabrication complexity, reproducibility, and tolerances, and quality control.

Cost: The device must be produced within the project's budget of $1,000, with careful consideration of material use. The design must stay within budget without compromising functionality and performance.

Design 1:

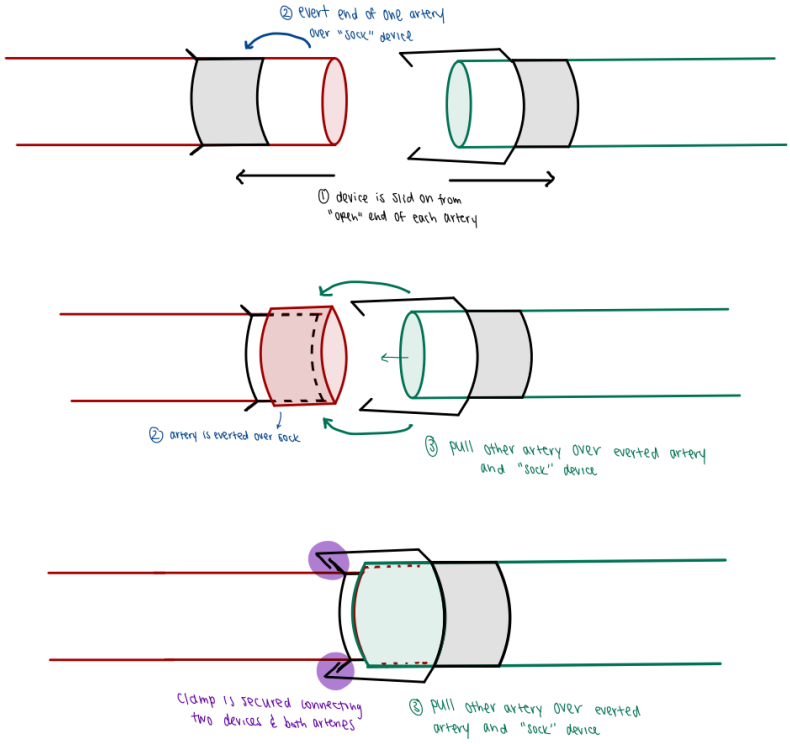

Figure 1: Sock clamp mechanism for sutureless arterial anastomosis.

Design Description: The sock clamp design facilitates arterial anastomosis by using a support sleeve to simplify vessel inversion and alignment. The device is positioned by sliding it onto the open ends of both arteries. One artery is then everted over the sock, exposing its endothelial surface. The opposing artery is pulled over the everted vessel and device, creating direct intima to intima contact between the two arterial ends. Finally, a clamp is secured over the overlap locking the arteries and device to complete the procedures. This approach eliminates the need for sutures, reduces implantation time, and promotes stable vessel contact for improved healing.

Efficiency: This design scored a ⅗ for effectiveness as is it easy to insert the end of the arteries into the two couplers. Once the arteries are everted, the device can simply be clamped together, removing the need for sutures, which are the most time-consuming factor in anastomosis. A significant limitation for the design is the fact that the design requires everting the artery over a fully expanded diameter (~3 mm). Everting the artery over a fully expanded device and then layering the opposing artery over will take more

time. Additionally, the clamping mechanism may pose difficulties if there is a variability in the thickness of the artery which may hinder an easy attachment.

Adjustability: This device scored a ⅕ for adjustability, as the rigid design that cannot be compressed easily to make everting the artery of the device easier. The rigid device will only perform at the diameter it was originally designed at.

Intima Contact: This design scored a 5⁄5 for intima contact since it involves everting one end fully and pulling the other artery over this everted position. This maximized intima to intima contact since all of the arterial contact is occurring between the inner lining of each artery. As well, the device avoids direct contact with the intima which can lead to clotting.

Durability: The device scored a ⅘ in durability since the bulk of the device is made from a single compact body. Potential issues may stem from the durability of the clamping mechanism, with the risk of fracturing in use.

Safety: This device ranked a ⅘ for safety since the clamping mechanism provides an added layer of security attaching the two devices together. When blood pressure achieves reading beyond 120 mmHg the device will still be able to withstand these extraneous pressures.

Manufacturability: This device scored a ⅘ in manufacturability since it is overall a uniform body that can be printed in one go. There is the risk of the clamps making manufacturing of the device more difficult due to their extended configuration.

Cost: This device scored a ⅘ for cost since it can be machined or 3D printed with biocompatible materials at a low cost. There may be an increase in price due to the complexity of some design components.

Design 2:

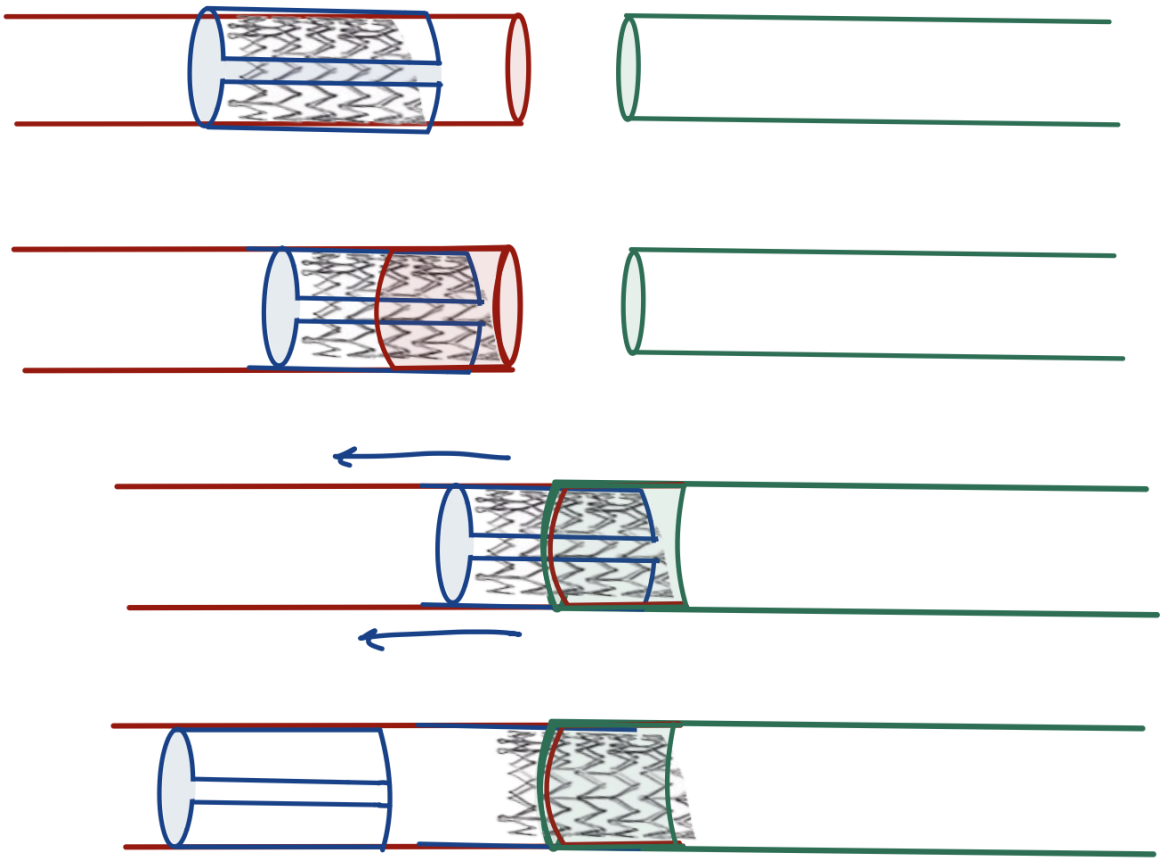

Figure 2: Expandable stent mechanism for sutureless arterial anastomosis.

Design Description: The design connects two arteries using a self expanding stent housed within a delivery device. The stent is first positioned within the lumen of one artery, after which the opposing artery is advanced over the exposed stent. As the stent is eventually deployed, it expands outward to secure both arterial ends against the mesh framework, creating consistent intima to intima contact. Once fully released, the stent maintains vessel alignment and patency without the need for sutures while the delivery device is withdrawn.

Efficiency: This device scored a ⅘ for efficiency since it only involves two components that will intact directly with one artery end as opposed to two. Only needing to attach a device to one end of the artery will decrease the amount of time of the procedure, and the expanding stent will further allow for the loading device to be removed quickly and easily.

Adjustability: This device scored a ⅘ for adjustability since the nitinol stent allows for easy deformation of the material. Initially the device will be loaded into a loader tube that will restrict the diameter of the stent to ~2.5 mm. Expecting the artery in the application is 3 mm, this will allow for easier eversion of the artery over the stent and attachment of the opposing artery over the other end. Once the loader tube is removed, the nitinol stent will expand to the diameter it was originally manufactured at and hold the artery open.

Intima Contact: This device scored a 5⁄5 for intima contact since it involves fully everting the proximal end and pulling the distal artery over the everted end. This maximizes intima to intima contact, as all of the arterial contact is occurring between the inner lining of each artery. Additionally, the device avoids direct contact with the intima, which can lead to clotting and biocompatibility issues.

Durability: This device scored a ⅗ for durability since the nitinol stent can be easily compressed. While this is a contributing factor to its adjustability, it will have to be machined in a configuration that still maintains mechanical strength in its fully expanded state and does not allow for easy deformation unless held by the loading device.

Safety: This device scored a ⅘ for safety since nitinol is a highly reputable and FDA approved material. The titanium oxide barrier that forms at the top layer of the material prevents nickel ion leaching.

Manufacturability: This device scored a ⅗ for manufacturability since the assembly, laser cutting, and electropolishing process for nitinol stents is more time demanding than the other design options.

Cost: This device scored a ⅗ due to the higher cost of nitinol . The nitinol material itself is not costly but the manufacturing process contributes to increased prices of the fully developed product.

Design 3:

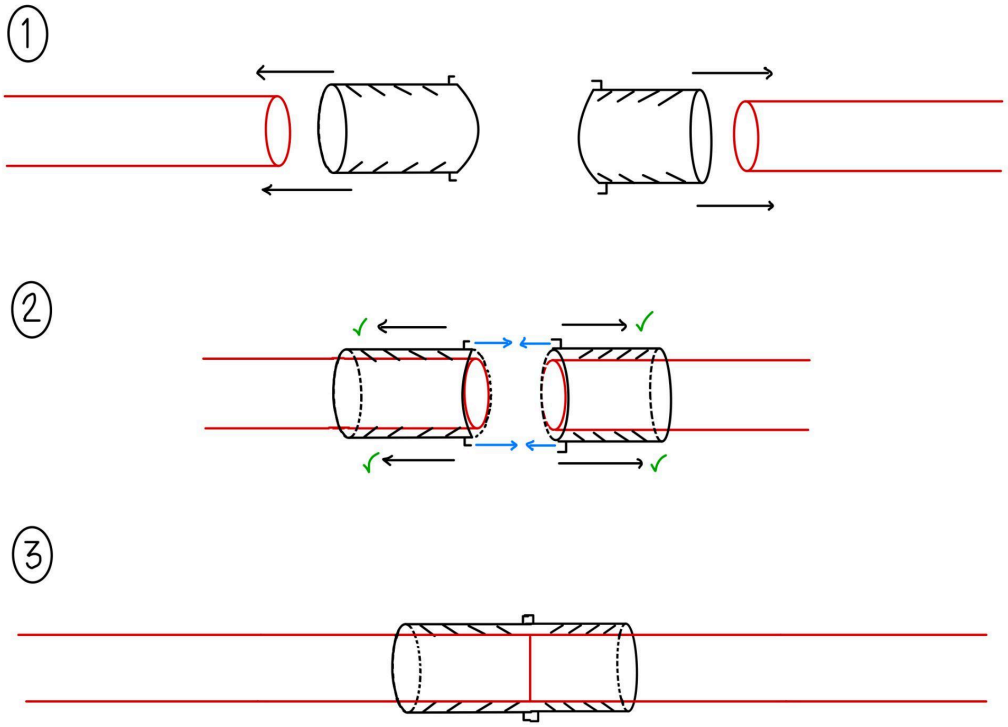

Figure 3: SpikeStent mechanism for sutureless arterial anastomosis.

Design Description: The SpikeStent design secures two arteries using a cylindrical stent with outward facing spikes that anchor the vessel walls. First, each arterial end is advanced over the side of the SpikeStent. The vessels are then approximated at the center where the spikes interlock with the arterial walls to establish stable intima to intima contact. Once both arteries are fully engaged, the device holds them in alignment, maintaining patency without the need for sutures. This approach leverages mechanical fixation to ensure consistent contact and reduce the risk of slippage at the anastomotic site.

Efficiency: This design scored a ⅖ for efficiency since the design poses difficulties when inserting the artery into the stent like structure. Since the artery will not have any outward pressure from fluid flow, pulling the rigid device over the limp vessel will pose a difficulty. The clamps may need to be secured with sutures as well which will add to the overall implantation time and further reduce efficiency.

Adjustability: This design scored a ⅛ for adjustability since it does not allow for any expandable diameter. The device remains rigid and the prongs lining the inner diameter will pose a safety threat of puncturing the arterial wall if the device is compressed.

Intima Contact: This device scored a ⅖, the lowest of the three designs, for intima contact. This design does not require the eversion of one artery end, which may increase efficiency, but allows for very minimal intima contact. With a simple end-to-end connection, overlapping surface area is minimized to just the cross-section of the vessel.

Durability: This device scored a ⅗ for durability due to the clamp mechanism and the prongs lining the interior of the design. Since the prongs will be thin in nature they are more at risk of breaking during manufacturing or application.

Safety: This device scored a ⅖ for safety since the prongs pose a threat of puncturing the arterial wall. This can impact hemodynamic and overall functionality of the artery. If the puncture were to also make contact with the intima it can promote clotting and thrombosis, posing very large safety risks.

Manufacturability: The device scored a ⅗ for manufacturability due to the complex nature of printing the inner diameter of the stent. Given the very small nature of the design it will also be difficult to file down the edges on the prongs to ensure they are not sharp enough to puncture the artery. This device would need to be machined with tight tolerances, further increasing the difficulty of manufacturing.

Cost: The device scored a ⅘ since it can be machined or 3D printed with biocompatible materials at a low cost. There may be an increase in price due to the complexity of some design components.

Appendix IV - SolidWorks Modeling Protocol: Rigid Tube

Software: SolidWorks

Material: AISI 316 Stainless Steel

1. Open Solidworks
2. Select New → Part
3. Select units:
    a. Bottom right corner → Units
    b. Select MMGS (millimeter, gram, second)
4. Select the Front Plane
5. Click Sketch
6. Select Center Circle
7. Draw two concentric circles from the origin:
    a. Inner circle
    b. Outer circle
8. Dimension the circles
    a. Inner diameter: 2.31 mm
    b. Outer diameter: 2.54 mm
9. Ensure both circles share the same center point (concentric constraint)
10. Exit the sketch
11. Select Features → Extruded Boss/Base
12. Set:
    a. Extrusion type: Blind
    b. Depth: 3.00 mm
13. Confirm the feature
14. In the FeatureManager design tree, right click: Material <not specified>
15. Select Edit Material
16. Navigate to: Steel → Stainless Steel
17. Select AISI 316
18. Click Apply, then Close

Appendix V - SolidWorks Modeling Protocol: Stent Design

Software: SolidWorks

Material: Nitinol (Nickel-Titanium Alloy)

1. Open Solidworks
2. Select New → Part
3. Select units:
    a. Bottom right corner → Units
    b. Select MMGS (millimeter, gram, second)
4. Select the Front Plane
5. Click Sketch
6. Select Center Circle
7. Draw one circle from the origin
8. Dimension the circle:
    a. Diameter: 3.00 mm
9. Exit the sketch
10. Select Surfaces → Extruded Surface
11. Set extrusion parameters:
    a. Type: Blind
    b. Depth: 3.00 mm
    c. Direction: Midplane
12. Confirm the feature
13. Select the bottom circular edge of the cylinder
14. Click Insert → Curve → Helix/Spiral
15. Define the helix using:
    a. Method = Height and Revolutions
    b. Height = 3.00 mm
    c. Revolutions = 0.125
    d. Direction = Clockwise
16. Confirm the helix
17. Create a plane normal to the start of the helix
18. Select the new plane
19. Click Sketch

20. Draw a rectangle
21. Dimension the rectangle width:
    a. Width = 0.28 mm
22. Fully define the sketch
23. Exit the sketch
24. Select Surfaces → Swept Surface
25. Set:
    a. Profile = rectangle sketch
    b. Path = helix
26. Confirm the surface strip
27. Select Surfaces → Offset Surface as needed to define lattice boundaries
28. Select Surfaces → Extend Surface to ensure complete intersections for trimming
29. Confirm operations
30. Select Surfaces → Trim Surface
31. Use intersecting surfaces to remove excess material
32. Retain one repeating diamond lattice segment
33. Confirm the trimmed geometry
34. Select Features → Thicken
35. Set thickness:
    a. Thickness = 0.05 mm
    b. Direction = Inward
36. Confirm
37. Select the cylindrical face
38. Click Insert → Reference Geometry → Axis
39. Create the central longitudinal axis
40. Select Features → Circular Pattern
41. Select the created axis as the pattern axis
42. Select the mirrored solid body to pattern
43. Set number of instances = 24
44. Enable Equal Spacing
45. Confirm the pattern
46. Select Features → Combine
47. Choose Add operation
48. Select all patterned bodies

49. Confirm to merge into a single solid body
50. In the FeatureManager tree, right click Material <not specified>
51. Select Edit Material
52. Navigate to appropriate Nitinol material library
53. Select Nitinol (Nickel-Titanium Alloy)
54. Click Apply, then Close

Appendix VI - Testing Protocol

Efficiency and Usability Testing

Efficiency and Usability testing is directed at establishing that the proposed model will efficiently reduce mean anastomosis time from the current standard (suture method). The time required for each procedure will be recorded, beginning when the artery in the ex vivo chicken thigh artery is first cut and ending when the surgeon determines the artery has been successfully anastomosed.

To account for variability in surgical expertise, multiple microsurgeons with varying levels of experience (novice, intermediate, and expert) will perform the procedure. Mean procedure time will be calculated for each experience group, and comparisons will be made across groups. A successful efficiency outcome will be defined as a mean procedure time of ≤20 minutes.

Following each procedure, surgeons will complete a 5-point Likert scale usability survey. A successful usability result will be defined as an average score of 4.0 or greater across responses.

Finally, the failure rate of the procedure will be recorded and compared to literature values for the traditional suture method. Failure is defined as an inability to successfully complete the anastomosis using the device, requiring the surgeon to abandon the device. A successful result will be defined as a failure rate of <10%. Additionally, surgeons will report their level of microsurgical experience to allow usability results to be stratified by experience level.

5.0 Likert Scale

Please rate the following statements regarding the usability of the arterial anastomosis device per the following scale.

1 - Strongly Disagree

2 - Disagree

3 - Neutral

4 - Agree

5 - Strongly Agree

- The device was intuitive to understand during initial use.
- The setup and preparation of the device were straightforward.
- The device was easy to handle during the anastomosis procedure.
- The device allowed precise control while performing the anastomosis.
- The steps required to complete the anastomosis were clear and logical.
- The device integrated smoothly into my normal surgical workflow.
- The device reduced the technical difficulty of performing the anastomosis.
- The time required to complete the anastomosis using this device was acceptable.

- I felt confident in the reliability of the device during the procedure.
- The device would be easy for surgeons to learn with minimal training.
- The device improved the overall efficiency of the procedure.
- I would consider using this device in future procedures.

Optional Open Response

- What aspects of the device worked particularly well?
- What aspects of the device should be improved?

Level of Microsurgical Experience:

- Novice (resident/limited microsurgical experience)
- Intermediate (trained surgeon with moderate microsurgical experience)
- Expert (fellowship-trained or highly experienced microsurgeon)

Patency, Leakage, % Stenosis Testing

Patency, leakage, and percent stenosis testing are aimed at ensuring that the device adequately achieves patency, prevents leakage, and maintains vessel openness following the procedure.

Patency will be determined by the openness and degree of expansion of the vessel following device implementation. Once the vessel has been anastomosed, a syringe pump will be used to pump a blue dye through the vessel at 80–120 mmHg. A successful deployment will achieve ≥95% patency, which will be measured using ImageJ following the procedure.

Leakage will be evaluated by pressurizing the vessel with blue dye at 80–120 mmHg and visually assessing dye escape at the anastomosis site. A control group consisting of sutured anastomoses without the device will be used to establish baseline leakage levels. Leakage from branch vessels will be identified and excluded from anastomosis leakage measurements to ensure accurate assessment of device performance. Leak grade will be determined using a 0–3 scale, where 0 indicates no leakage and 3 indicates vessel rupture. In addition to the grading scale, leakage severity will be qualitatively assessed, and consultation with a microsurgeon may be used to determine whether observed leakage is clinically significant. A trial will be considered successful with grade 0 leakage following 80–120 mmHg pressurization.

Percent restenosis will also be measured using ImageJ following the procedure to determine the percentage of lumen narrowing. A trial will be considered successful with <20% lumen narrowing.

Materials and Equipment

- Ex vivo chicken thigh arteries (fresh, similar diameter across samples)
- Anastomosis device prototypes (n=5)
- Standard surgical instruments (scissors, forceps, scalpel, needle holder, sutures as needed)
- Stopwatch or digital timer
- MTS machine (for tensile testing)
- Syringe pump (calibrated for 80-120 mmHg)
- Blue dye solution (contrast agent for visualization)
- Imaging setup (camera and ImageJ analysis software)
- Likert-scale usability questionnaire (1-5 scale)
- Data recording sheet or digital spreadsheet

Testing Plan Procedure

Five independent anastomosis trials will be conducted using ex vivo chicken thigh arteries. Each trial will consist of one arterial pair and one device prototype. Trials will be performed by surgeons with varying experience levels when available. All performance metrics (efficiency, usability, failure rate, handling, leakage, patency, stenosis, and mechanical strength) will be collected from each individual trial. Prior to each trial, participating users will be briefed on the testing protocol, evaluation metrics, and success criteria to ensure consistent implementation across trials.

Step 1: Anastomosis

1. Begin trial preparation by setting up the testing area and ensuring all instruments are ready.
2. Assign one independent trial per artery (five trials total).
3. Start the timer when the artery is first cut.
    - Split measurements will be taken through this testing. In all, we will be analyzing the time it takes to complete the procedure, however, separate times will be collected that measure the duration of each element. This would include: looping first artery through stent, everting first artery over stent, overlaying opposing artery, and leakage testing.
4. Perform the anastomosis using the proposed spring/stent device:
    - Fit the device around the proximal artery end
    - Evert the proximal artery over the stent/spring
    - Sleeve the distal end over the interiorly exposed proximal end
    - (Optional, at discretion of surgeon) Secure with a circumferential suture
        i. Take note of instances where securing suture is needed
5. Stop the timer when the surgeon determines that the anastomosis is complete and functional.

- Procedures exceeding 30 minutes or requiring abandonment of the device will be classified as failures.

6. Record total procedure time.
    - Procedure time will be measured using two timers: one device will record step-by-step task durations, while another device will record total procedure time from the start of device deployment to completion of the anastomosis.
    - Success criterion: Completion time ≤ 20 minutes for novice users (residents or surgeons with limited microsurgical experience). Procedure time will also be compared across novice, intermediate, and expert users to assess usability and learning curve.
7. The surgeon and assistant completes the 5-point usability Likert scale regarding device handling, clarity, and intuitiveness.
    - Success criterion: Average score ≥ 4.0.
8. Record failure occurrence, if the device cannot complete the anastomosis or leakage prevents functional bonding.
    - Success criterion: Failure rate < 10%.

Step 2: Patency, Leakage, and Stenosis Testing

1. Following anastomosis, connect the artery to a syringe pump set to deliver blue dye at 80-120 mmHg.
2. Observe dye flow through the vessel.
3. Patency: Capture images of the anastomosis region. Quantify vessel lumen openness in ImageJ to determine the patency percentage.
    - Success criterion: ≥ 95% patency.
4. Leakage: Visually grade leakage according to the following:
    - 0: No leaks
    - 1: Minor leak
    - 2: Moderate leak
    - 3: Burst/major leak
    - Success criterion: Grade 0 at 80–120 mmHg pressure. The vessel will additionally be tested at 160–180 mmHg to assess leakage under elevated pressure conditions.
5. Percent restenosis (lumen narrowing): Analyze lumen diameter before and after procedure in ImageJ. Calculate percent narrowing.
    - Success criterion: < 20% restenosis.

Step 3: Data Collection

Ensure record of the following for each of the five trials:

- Procedure time (minutes)
- Likert usability score (1-5)
- Success/failure
- Failure force (g) from MTS
- Misfire event (yes/no)
- Leakage grade (0–3)
- Percent stenosis (%)
    - For percent stenosis, measure length of intima overlap
    - Could measure diameter before and after implantation of the device to determine patency or stenosis, etc.

Step 4: Analysis and Reporting

- Report each metric with mean ± standard deviation.
- Compare performance to literature benchmarks for standard suturing methods.
- Determine pass/fail outcome for each criterion.
- Summarize design feasibility based on combined technical and user performance metrics.

Appendix VII - Cuff Fabrication Plan

Cuff Fabrication Kit

Materials

- Afoxsos 24 Pc Stainless Steel Strips Shim Stock Metal Shims 1in. x 6 in., Assortment 8 Thickness Sizes Thin Metal Sheet
- Sharpie marker
- Straight edge
- Foot-operated shear (guillotine shear)
- Forceps

Procedure

1. Select the appropriate shim stock thickness from the kit for the desired fit tolerance.
2. Using a Sharpie and straight edge, mark the cut line on the shim stock. The marked length corresponds to the desired diameter of the finished rolled cuff once the strip is wrapped around itself, so confirm the length-to-diameter relationship before cutting.
3. Position the stock under the guillotine shear blade, aligning the marked cut line with the blade edge. Actuate the foot pedal to complete the cut. Verify the cut edge is straight and clean before proceeding.
4. Using forceps, grip one end of the cut strip and roll it tightly into a cuff/loop. Maintain consistent tension throughout the roll to avoid gaps or uneven overlap.

Notes

- Double-check the marked length against the target diameter before cutting, since this determines the final fit.
- A clean shear cut is critical; a skewed edge will cause the rolled cuff to sit unevenly.
- Forceps give better control than fingers for tight-radius rolling, especially on thinner stock.

Appendix VIII - Nitinol Spring Sourcing

Kellogg's Research Lab

- Kellogg's Research Labs is an innovative company focused on Nitinol product prototyping and development. They offer most varieties of Shape Memory Alloy online.
- Nitinol Springs of varying length/inner diameter were purchased from Kellogg's Research Lab
- See https://www.kelloggsresearchlabs.com/ for more information